JOURNAL OF ENZYME INHIBITION AND MEDICINAL CHEMISTRY
2018, VOL. 33, NO. 1, 1108–1124
https://doi.org/10.1080/14756366.2018.1480615

Taylor & Francis
Taylor & Francis Group

RESEARCH PAPER

OPEN ACCESS Check for updates

Synthesis, biological evaluation, and molecular modelling studies of potent human neutrophil elastase (HNE) inhibitors

Maria Paola Giovannoni[a], Igor A. Schepetkin[b], Mark T. Quinn[b], Niccolò Cantini[a], Letizia Crocetti[a], Gabriella Guerrini[a], Antonella Iacovone[a], Paola Paoli[c], Patrizia Rossi[c], Gianluca Bartolucci[a], Marta Menicatti[a] and Claudia Vergelli[a]

[a]NEUROFARBA, Pharmaceutical and Nutraceutical Section, University of Florence, Sesto Fiorentino, Italy; [b]Department of Microbiology and Immunology, Montana State University, Bozeman, MT, USA; [c]Department of Industrial Engineering, University of Florence, Florence, Italy

ABSTRACT

We report the synthesis and biological evaluation of a new series of 3- or 4-(substituted)phenylisoxazolones as HNE inhibitors. Due to tautomerism of the isoxazolone nucleus, two isomers were obtained as final compounds (2-NCO and 5-OCO) and the 2-NCO derivatives were the most potent with IC_{50} values in the nanomolar range (20–70 nM). Kinetic experiments indicated that 2-NCO **7d** and 5-OCO **8d** are both competitive HNE inhibitors. Molecular modelling on **7d** and **8d** suggests for the latter a more crowded region about the site of the nucleophilic attack, which could explain its lowered activity. In addition molecular dynamics (MD) simulations showed that the isomer **8d** appears more prone to form H-bond interactions which, however, keep the reactive sites quite distant for the attack by Ser195. By contrast the amide **7d** appears more mobile within the active pocket, since it makes single H-bond interactions affording a favourable orientation for the nucleophilic attack.

ARTICLE HISTORY
Received 6 April 2018
Revised 21 May 2018
Accepted 21 May 2018

KEYWORDS
Isoxazol-5(2H)-one; HNE; molecular modelling; stability

Introduction

Proteases are enzymes implicated in cellular reactions involving the cleavage of protein substrates[1]. Serine proteases are characterised by the presence of a serine residue at the active site[2]. They are divided into four classes: chymotrypsin, subtilisin, carboxypeptidase Y, and caseinolytic protease[3]. Human neutrophil elastase (HNE), proteinase 3 (PR3), cathepsin G, and the recently discovered NSP4[4] are serine proteases belonging to the chymotrypsin family and represent neutrophil serine proteases (NSP)[5,6]. NSP are synthesised and expressed in neutrophil azurophilic granules. Neutrophils play a pivotal role in host defence, inflammation and tissue remodelling, and HNE is a key mediator of neutrophil-driven inflammation[7].

HNE is a small, basic, and soluble glycoprotein of about 30 kDa[8] that performs many functions in our body. For example, HNE is involved in the maintenance of tissue homeostasis; it degrades a variety of structural proteins of the extracellular matrix, such as elastin, fibronectin, collagen, proteoglycan, and laminin; and it repairs damaged tissue[9]. Moreover, HNE plays an important and dual role in inflammation by degrading pro-inflammatory cytokines to reduce the intensity of the inflammation but also increasing the secretion of pro-inflammatory factors[10]. In the case of infection, HNE plays as an intracellular function in destroying phagocytosed pathogens, as well as an extracellular function through the formation of neutrophil extracellular traps, which can trap and kill microorganisms[11,12]. The powerful HNE activity is tightly controlled by the presence of extracellular neutralizing endogenous serine protease inhibitors, such as α-1 antitrypsin, secretory leucocyte protease inhibitor (SLPI), and elafin[13]. α1-Antitrypsin is a water-soluble glycoprotein classified as systemic HNE inhibitor that is synthesised in the liver and is particularly abundant in the lungs[14]. In contrast, SLPI and elafin are classified as alarm inhibitors because they are produced and released directly into the airway epithelium in response to the release of cytokines, regulating the immune response and inflammatory processes[15–17]. Under physiological conditions, the balance between protease and anti-protease supports the maintenance of tissue homeostasis. However, if this balance fails, excessive HNE activity can cause tissue the damage associated with some serious chronic diseases[4,6]. Among the pathologies associated with increased HNE activity are adult respiratory distress syndrome (ARDS)[18], chronic obstructive pulmonary disease (COPD)[19,20], cystic fibrosis (CF)[21,22], and other disorders with an inflammatory component, such as rheumatoid arthritis[23], atherosclerosis[24], psoriasis, and dermatitis[25]. Recently, it was demonstrated that HNE is also implicated in the progression of non-small cell lung cancer[26].

Although a large number of molecules have been reported as HNE inhibitors[27,28], only two drugs are currently available for clinical use: Prolastin (purified α1-AT), a peptide drug synthesised by recombinant DNA techniques[29] and used for the treatment of α1-antitripsin deficiency (AATD)[30], and Sivelestat (Elaspol®100), a non-peptide low molecular weight compound, belonging to the second generation of HNE inhibitors[31]. Sivelestat has an $IC_{50} = 44$ nM and is currently marketed only in Japan and South Korea[32,33] (Figure 1). AZD9668 (Alvelestat, AstraZeneca)[34] and BAY 85-8501 (Bayer HealthCare)[35] are two potent HNE inhibitors, belonging to the third and fifth generations of HNE inhibitors[31],

CONTACT Letizia Crocetti letizia.crocetti@unifi.it Dipartimento di NEUROFARBA, Via Ugo Schiff 6, Sesto Fiorentino 50019 Firenze, Italy

Supplemental data for this article can be accessed here.

© 2018 The Author(s). Published by Informa UK Limited, trading as Taylor & Francis Group.
This is an Open Access article distributed under the terms of the Creative Commons Attribution License (http://creativecommons.org/licenses/by/4.0/), which permits unrestricted use, distribution, and reproduction in any medium, provided the original work is properly cited.

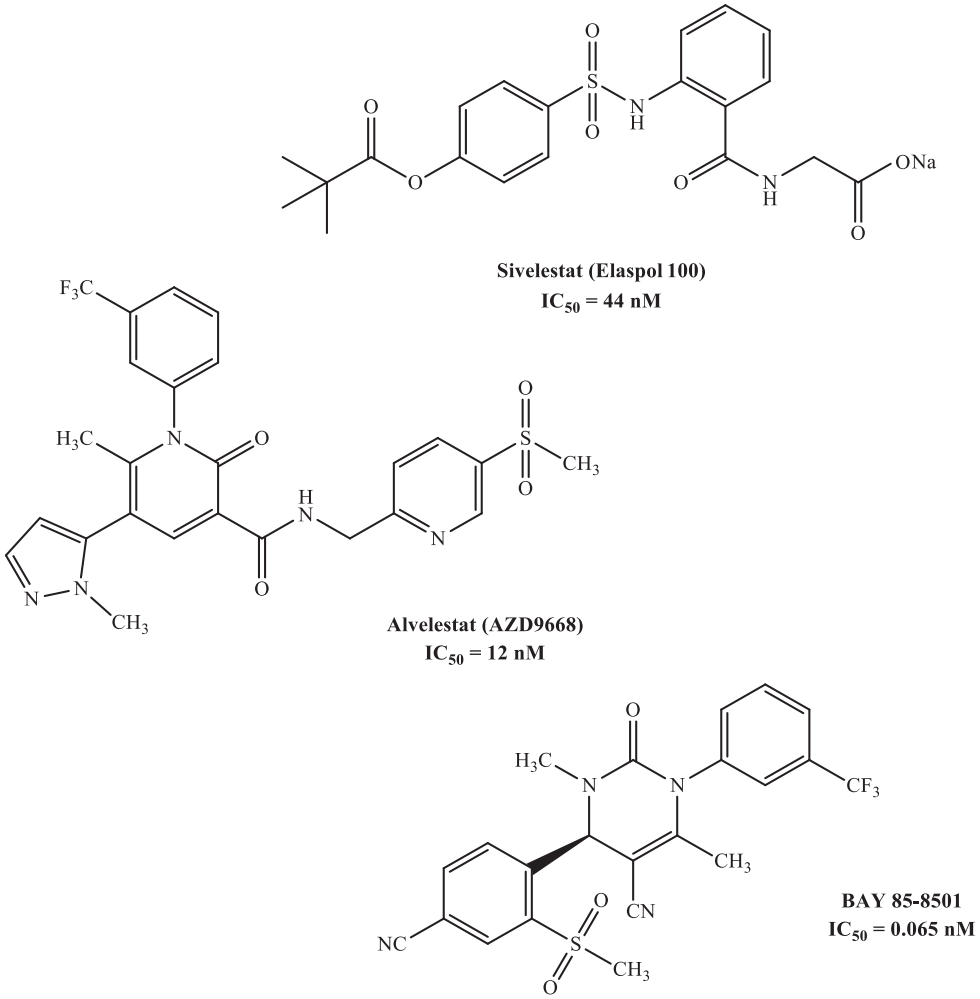

Figure 1. Potent HNE inhibitors.

respectively, that have recently reached Phase II of clinical trials for COPD, CF, and BE (Figure 1).

In recent research focused on the development of new HNE inhibitors, we investigated various bicyclic scaffolds, such as indazole[36,37], indole[38], and cinnolinone[39], compounds. The most interesting inhibitors were effective in the nanomolar range, with a potency comparable to Sivelestat. Subsequently, we focused our research on the design and synthesis of monocyclic derivatives with an isoxazol-*5*(*2H*)-one core, and the first series of 3/4-alkyl-(di)substituted isoxazolones was recently published[40]. We report here the synthesis of a new series of isoxazolone derivatives bearing a (substituted)phenyl at positions *3* and *4* and biological evaluation of their HNE inhibitory activity.

Material and methods

All melting points were determined on a Büchi apparatus (New Castle, DE) and are uncorrected. Extracts were dried over Na_2SO_4, and the solvents were removed under reduced pressure. Merck F-254 commercial plates (Merck, Durham, NC) were used for analytical TLC to follow the course of reactions. Silica gel 60 (Merck 70–230 mesh, Merck, Durham, NC) was used for column chromatography. ^{1}H NMR, ^{13}C NMR, HSQC, HMBC, and NOESY bidimensional spectra were recorded on an Avance 400 instrument (Bruker Biospin Version 002 with SGU, Bruker Inc., Billerica, MA). Chemical shifts (δ) are reported in ppm to the nearest 0.01 ppm using the solvent as an internal standard. Coupling constants (*J* values) are given in Hz and were calculated using TopSpin 1.3 software (Nicolet Instrument Corp., Madison, WI) and are rounded to the nearest 0.1 vHz. Mass spectra (*m/z*) were recorded on an ESI-TOF mass spectrometer (Brucker Micro TOF, Bruker Inc., Billerica, MA), and reported mass values are within the error limits of ±5 ppm mass units. Microanalyses indicated by the symbols of the elements or functions were performed with a Perkin–Elmer 260 elemental analyser (PerkinElmer, Inc., Waltham, MA) for C, H, and N, and the results were within ±0.4% of the theoretical values, unless otherwise stated. Reagents and starting material were commercially available.

Chemistry

3-Methyl-2-(3-methylbenzyl)-4-phenylisoxazol-5(2H)-one (2)

A mixture of the appropriate intermediate (**1a**[41]) (0.57 mmol), K_2CO_3 (1.14 mmol), and 1-(chloromethyl)-3-methylbenzene (0.86 mmol) in 2 ml of anhydrous acetonitrile was stirred at reflux for 2 h. After cooling, the mixture was concentrated *in vacuo*, diluted with ice-cold water (10 ml), and extracted with ethyl acetate (3 × 15 ml). The organic phase was dried over sodium sulphate and the solvent was evaporated *in vacuo* to afford the final compound **2**, which was purified by column chromatography using cyclohexane/ethyl acetate 2:1 as eluent. Yield =57%; oil. ^{1}H NMR ($CDCl_3$-d_1) δ 2.35 (s, 6H, 2 × CH_3), 4.79 (s, 2H, CH_2), 7.07–7.14 (m, 3H, Ar), 7.22–7.28 (m, 2H, Ar), 7.38 (t, 2H, Ar, J = 7.8 Hz), 7.45 (d, 2H, Ar, J = 7.2 Hz). ^{13}C NMR ($CDCl_3$-d_1) δ 12.44 (CH_3), 21.63 (CH_3), 54.90 (CH_2), 103.58 (C), 125.16 (CH), 127.17 (CH), 128.21 (CH),

128.58 (CH), 128.82 (CH), 128.90 (CH), 129.40 (CH), 129.77 (C), 133.45 (C), 138.75 (C), 158.65 (C), 169.53 (C). ESI-MS calcd. for $C_{18}H_{17}NO_2$, 279.33; found: *m/z* 280.13 $[M+H]^+$. Anal. $C_{18}H_{17}NO_2$ (C, H, N).

General procedure for compounds (3a–c)

To a suspension of the appropriate 4-substituted benzensulfonyl chloride (0.16 mmol) in 3 ml of anhydrous pyridine, 0.79 mmol of intermediate **1a**[41] was added. The mixture was stirred at room temperature for 4 h. The solvent was concentrated *in vacuo* to afford the final compounds **3a–c** which were purified by column chromatography using cyclohexane/ethyl acetate in different ratio (2:1 for **3a**, 4:1 for **3b**) or toluene/ethyl acetate 9:1 for **3c** as eluents.

2-((4-Hydroxyphenyl)sulfonyl)-3-methyl-4-phenylisoxazol-5(2H)-one (3a). Yield = 30%; mp = 50–51 °C (EtOH). ^{1}H NMR ($CDCl_3$-d_1) δ 2.57 (s, 3H, CH_3), 6.93 (d, 2H, Ar, J = 8.8 Hz), 7.30–7.40 (m, 5H, Ar), 7.78 (d, 2H, Ar, J = 8.8 Hz). ^{13}C NMR ($CDCl_3$-d_1) δ 14.59 (CH_3), 113.94 (C), 116.39 (CH), 121.92 (C), 126.91 (C), 128.77 (CH), 128.87 (CH), 129.19 (CH), 131.88 (CH), 158.94 (C), 162.88 (C), 168.80 (C). ESI-MS calcd. for $C_{16}H_{13}NO_5S$, 331.34; found: *m/z* 332.05 $[M+H]^+$. Anal. $C_{16}H_{13}NO_5S$ (C, H, N).

4-((3-Methyl-5-oxo-4-phenylisoxazol-2(5H)-yl)sulfonyl)phenyl pivalate (3b). Yield = 15%; mp = 115–116 °C (EtOH). ^{1}H NMR ($CDCl_3$-d_1) δ 1.35 (s, 9H, $C(CH_3)_3$), 2.58 (s, 3H, CH_3), 7.26 (d, 2H, Ar, J = 8.0 Hz), 7.32 (d, 2H, Ar, J = 8.6 Hz), 7.35–7.40 (m, 3H, Ar), 7.95 (d, 2H, Ar, J = 8.6 Hz). ^{13}C NMR ($CDCl_3$-d_1) δ 14.50 (CH_3), 26.97 (CH_3), 29.37 (C), 39.36 (C), 114.27 (C), 122.81 (CH), 127.03 (C), 128.45 (CH), 128.81 (CH), 129.11 (CH), 130.39 (CH), 130.97 (CH), 156.83 (C), 157.77 (C), 167.45 (C), 175.75 (C). ESI-MS calcd. for $C_{21}H_{21}NO_6S$, 415.46; found: *m/z* 416.11 $[M+H]^+$. Anal. $C_{21}H_{21}NO_6S$ (C, H, N).

N-(4-((3-methyl-5-oxo-4-phenylisoxazol-2(5H)-yl)sulfonyl)phenyl)pivalamide (3c). Yield = 72%; mp = 153–155 °C (EtOH). ^{1}H NMR ($CDCl_3$-d_1) δ 1.30 (s, 9H, $C(CH_3)_3$), 2.58 (s, 3H, CH_3), 7.26 (d, 1H, Ar, J = 6.8 Hz), 7.36–7.42 (m, 4H, Ar), 7.70 (exch br s, 1H, NH), 7.79 (d, 2H, Ar, J = 8.8 Hz), 7.84 (d, 2H, Ar, J = 8.8 Hz). ^{13}C NMR ($CDCl_3$-d_1) δ 14.61 (CH_3), 27.42 (CH_3), 44.65 (C), 113.95 (C), 119.39 (CH), 125.36 (C), 125.85 (CH), 128.43 (CH), 128.81 (CH), 128.97 (CH), 129.88 (CH), 130.68 (CH), 130.91 (CH), 134.00 (C), 144.98 (C), 158.06 (C), 165.00 (C), 177.20 (C). ESI-MS calcd. for $C_{21}H_{22}N_2O_5S$, 414.47; found: *m/z* 415.13 $[M+H]^+$. Anal. $C_{21}H_{22}N_2O_5S$ (C, H, N).

General procedure for compounds (4a–h, 4n–t)

To a suspension of the appropriate substrates **1a–e** (**1a**[41], **1b**[42], **1c,d**[43], and **1e**[44]) (0.86 mmol) in 10 ml of anhydrous THF, 1.72 mmol of sodium hydride (60% dispersion in mineral oil), and 1.03 mmol of the appropriate acyl/aroyl chloride were added. The mixture was stirred at room temperature overnight. The solvent was concentrated *in vacuo* to obtain the final compounds **4a–h** and **4n–t** which were purified by column chromatography using hexane/ethyl acetate (5:1 for **4a**,**c**,**d**; 5:2 for **4e**,**g**), cyclohexane/ethyl acetate (1:1 for **4f**; 3:1 for **4t**; 4:1 for **4h**; 5:1 for **4o–s**; 6:1 for **4n**), or toluene/ethyl acetate 9.5:0.5 (for **4b**) as eluents.

3-Methyl-2-(3-methylbenzoyl)-4-phenylisoxazol-5(2H)-one (4a). Yield = 52%; mp = 85–88 °C (EtOH). ^{1}H NMR ($CDCl_3$-d_1) δ 2.43 (s, 3H, m-CH_3-Ph), 2.79 (s, 3H, CH_3), 7.35–7.40 (m, 3H, Ar), 7.43–7.51 (m, 4H, Ar), 7.70–7.75 (m, 2H, Ar). ^{13}C NMR ($CDCl_3$-d_1) δ 15.09 (CH_3), 21.58 (CH_3), 108.39 (C), 127.08 (CH), 127.62 (C), 128.28 (CH), 128.50 (CH), 128.81 (CH), 129.08 (CH), 130.28 (CH), 131.14 (C), 134.07 (CH), 138.32 (C), 154.62 (C), 163.79 (C), 165.90 (C). IR (υ) = 1690 cm^{-1} (CO amide), 1750 cm^{-1} (CO ester). ESI-MS calcd. for $C_{18}H_{15}NO_3$, 293.32; found: *m/z* 294.11 $[M+H]^+$. Anal. $C_{18}H_{15}NO_3$ (C, H, N).

2-(Cyclopropanecarbonyl)-3-methyl-4-phenylisoxazol-5(2H)-one (4b). Yield = 63%; mp = 83–86 °C (EtOH). ^{1}H NMR (DMSO-d_6) δ 1.02–1.07 (m, 2H, CH_2 cC_3H_5), 1.09–1.15 (m, 2H, CH_2 cC_3H_5), 2.36–2.41 (m, 1H, CH cC_3H_5), 2.58 (s, 3H, CH_3), 7.35–7.41 (m, 1H, Ar), 7.43–7.48 (m, 4H, Ar). ^{13}C NMR (DMSO-d_6) δ 10.82 (CH_2), 13.25 (CH_3), 15.14 (CH), 106.28 (C), 128.25 (C), 128.58 (CH), 129.10 (CH), 129.35 (CH), 154.69 (C), 166.05 (C), 169.02 (C). IR (υ) = 1695 cm^{-1} (CO amide), 1755 cm^{-1} (CO ester). ESI-MS calcd. for $C_{14}H_{13}NO_3$, 243.26; found: *m/z* 244.09 $[M+H]^+$. Anal. $C_{14}H_{13}NO_3$ (C, H, N).

3-Methyl-2-(4-methylbenzoyl)-4-phenylisoxazol-5(2H)-one (4c). Yield = 35%; mp = 134–136 °C (EtOH). ^{1}H NMR ($CDCl_3$-d_1) δ 2.51 (s, 3H, p-CH_3-Ph), 2.87 (s, 3H, CH_3), 7.38 (d, 2H, Ar, J = 8.0 Hz), 7.43–7.48 (m, 1H, Ar), 7.51–7.58 (m, 4H, Ar), 7.92 (d, 2H, Ar, J = 8.4 Hz). ^{13}C NMR ($CDCl_3$-d_1) δ 15.37 (CH_3), 22.02 (CH_3), 108.19 (C), 127.85 (C), 128.46 (CH), 128.59 (CH), 128.95 (CH), 129.19 (CH), 128.19 (CH), 130.28 (CH), 144.55 (C), 154.60 (C), 158.00 (C), 163.62 (C), 166.13 (C). IR (υ) = 1672 cm^{-1} (CO amide), 1755 cm^{-1} (CO ester). ESI-MS calcd. for $C_{18}H_{15}NO_3$, 293.32; found: *m/z* 294.11 $[M+H]^+$. Anal. $C_{18}H_{15}NO_3$ (C, H, N).

3-Methyl-2-(2-methylbenzoyl)-4-phenylisoxazol-5(2H)-one (4d). Yield = 42%; mp = 99–100 °C (EtOH). ^{1}H NMR ($CDCl_3$-d_1) δ 2.47 (s, 3H, o-CH_3-Ph), 2.85 (s, 3H, CH_3), 7.32 (d, 2H, Ar, J = 6.8 Hz), 7.40–7.49 (m, 7H, Ar). ^{13}C NMR ($CDCl_3$-d_1) δ 15.37 (CH_3), 20.22 (CH_3), 108.95 (C), 126.27 (CH), 128.10 (C), 128.74 (CH), 129.14 (CH), 129.43 (CH), 129.60 (CH), 131.53 (CH), 132.10 (CH), 132.52 (C), 137.22 (C), 153.99 (C), 164.91 (C), 166.31 (C). IR (υ) = 1688 cm^{-1} (CO amide), 1767 cm^{-1} (CO ester). ESI-MS calcd. for $C_{18}H_{15}NO_3$, 293.32; found: *m/z* 294.11 $[M+H]^+$. Anal. $C_{18}H_{15}NO_3$ (C, H, N).

3-Methyl-4-phenyl-2-(3-(trifluoromethyl)benzoyl)isoxazol-5(2H)-one (4e). Yield = 42%; mp = 96–97 °C (EtOH). ^{1}H NMR ($CDCl_3$-d_1) δ 2.85 (s, 3H, CH_3), 7.40–7.45 (m, 1H, Ar), 7.48–7.54 (m, 4H, Ar), 7.69 (t, 1H, Ar, J = 8.0 Hz), 7.90 (d, 1H, Ar, J = 7.8 Hz), 8.15 (d, 1H, Ar, J = 8.0 Hz), 8.20 (s, 1H, Ar). ^{13}C NMR ($CDCl_3$-d_1) δ 15.61 (CH_3), 109.53 (C), 125.39 (C), 127.34 (CH), 127.38 (C), 127.84 (CH), 129.33 (CH), 129.49 (CH), 129.63 (CH), 129.71 (CH), 130.28 (C), 131.69 (C), 132.75 (CH), 133.47 (CH), 154.88 (C), 162.74 (C), 166.07 (C). ^{19}F NMR ($CDCl_3$-d_1) δ − 62.82. IR (υ) = 1689 cm^{-1} (CO amide), 1738 cm^{-1} (CO ester). ESI-MS calcd. for $C_{18}H_{12}F_3NO_3$, 347.29; found: *m/z* 348.08 $[M+H]^+$. Anal. $C_{18}H_{12}F_3NO_3$ (C, H, N).

3-Methyl-2-(3-(methylsulfonyl)benzoyl)-4-phenylisoxazol-5(2H)-one (4f). Yield = 15%; mp = 185–186 °C (EtOH). ^{1}H NMR ($CDCl_3$-d_1) δ 2.83 (s, 3H, CH_3), 3.13 (s, 3H, CH_3SO_2), 7.40–7.45 (m, 1H, Ar), 7.48–7.55 (m, 4H, Ar), 7.75 (t, 1H, Ar, J = 8.0 Hz), 8.19 (d, 2H, Ar, J = 7.6 Hz), 8.46 (s, 1H, Ar). ^{13}C NMR ($CDCl_3$-d_1) δ 14.98 (CH_3), 44.52 (CH_3), 109.12 (C), 127.11 (C), 128.84 (CH), 128.93 (CH), 129.02 (CH), 129.75 (CH), 131.47 (CH), 132.84 (C), 134.47 (CH), 141.35 (C), 154.22 (C), 161.55 (C), 165.36 (C). ESI-MS calcd. for $C_{18}H_{15}NO_5S$, 357.38; found: *m/z* 358.07 $[M+H]^+$. Anal. $C_{18}H_{15}NO_5S$ (C, H, N).

3-(3-Methyl-5-oxo-4-phenyl-2,5-dihydroisoxazole-2-carbonyl)benzonitrile (4g). Yield = 7%; mp = 118–119 °C (EtOH). ^{1}H NMR ($CDCl_3$-d_1) δ 2.83 (s, 3H, CH_3), 7.45–7.55 (m, 5H, Ar), 7.67 (t, 1H, Ar,

$J = 7.2$ Hz), 7.89 (d, 1H, Ar, $J = 6.4$ Hz), 8.16 (d, 1H, Ar, $J = 7.6$ Hz), 8.20 (s, 1H, Ar). ^{13}C NMR ($CDCl_3$-d_1) δ 14.94 (CH_3), 107.22 (C), 112.76 (C), 118.63 (C), 127.98 (CH), 128.67 (CH), 128.91 (CH), 129.54 (CH), 130.71 (CH), 131.86 (CH), 134.54 (C), 134.95 (C), 135.62 (CH), 139.52 (C), 157.64 (C), 165.87 (C). ESI-MS calcd. for $C_{18}H_{12}N_2O_3$, 304.30; found: *m/z* 305.09 $[M+H]^+$. Anal. $C_{18}H_{12}N_2O_3$ (C, H, N).

4-(3-Methyl-5-oxo-4-phenyl-2,5-dihydroisoxazole-2-carbonyl)benzonitrile (4h). Yield = 46%; mp = 178–180 °C dec. (EtOH). ^{1}H NMR ($CDCl_3$-d_1) δ 2.82 (s, 3H, CH_3), 7.37–7.42 (m, 1H, Ar), 7.45–7.50 (m, 4H, Ar), 7.80 (d, 2H, Ar, $J = 8.4$ Hz), 8.00 (d, 2H, Ar, $J = 8.4$ Hz). ^{13}C NMR ($CDCl_3$-d_1) δ 14.94 (CH_3), 109.39 (C), 116.49 (C), 117.69 (C), 127.10 (C), 128.85 (CH), 128.93 (CH), 129.03 (CH), 130.41 (CH), 132.32 (CH), 135.19 (C), 154.20 (C), 161.73 (C), 165.45 (C). ESI-MS calcd. for $C_{18}H_{12}N_2O_3$, 304.30; found: *m/z* 305.09 $[M+H]^+$. Anal. $C_{18}H_{12}N_2O_3$ (C, H, N).

2-(Cyclopropanecarbonyl)-3,4-diphenylisoxazol-5(2H)-one (4n). Yield = 21%; mp = 100–103 °C (EtOH). ^{1}H NMR ($CDCl_3$-d_1) δ 1.06–1.11 (m, 2H, CH_2 cC_3H_5), 1.16–1.21 (m, 2H, CH_2 cC_3H_5), 1.80–1.86 (m, 1H, CH cC_3H_5), 7.17–7.22 (m, 2H, Ar), 7.31–7.40 (m, 5H, Ar), 7.39 (d, 1H, Ar, $J = 7.2$ Hz), 7.46 (d, 2H, Ar, $J = 7.6$ Hz). ^{13}C NMR ($CDCl_3$-d_1) δ 10.39 (CH_2), 12.51 (CH), 103.59 (C), 128.03 (CH), 128.31 (CH), 128.37 (CH), 128.72 (CH), 129.16 (CH), 129.84 (CH), 134.92 (C), 142.60 (C), 170.20 (C), 180.73 (C). ESI-MS calcd. for $C_{19}H_{15}NO_3$, 305.33; found: *m/z* 306.11 $[M+H]^+$. Anal. $C_{19}H_{15}NO_3$ (C, H, N).

4-Methyl-2-(3-methylbenzoyl)-3-phenylisoxazol-5(2H)-one (4o). Yield = 27%; oil. ^{1}H NMR ($CDCl_3$-d_1) δ 1.96 (s, 3H, CH_3), 2.40 (s, 3H, m-CH_3-Ph), 7.32–7.40 (m, 2H, Ar), 7.44–7.50 (m, 5H, Ar), 7.70 (d, 2H, Ar, $J = 6.8$ Hz). ^{13}C NMR ($CDCl_3$-d_1) δ 7.57 (CH_3), 21.63 (CH_3), 105.74 (C), 127.37 (CH), 128.01 (CH), 128.33 (CH), 128.67 (CH), 128.82 (C), 130.51 (CH), 130.60 (CH), 131.07 (C), 134.31 (CH), 138.46 (C), 156.85 (C), 165.24 (C), 169.02 (C). ESI-MS calcd. for $C_{18}H_{15}NO_3$, 293.32; found: *m/z* 294.11 $[M+H]^+$. Anal. $C_{18}H_{15}NO_3$ (C, H, N).

2-(Cyclopropanecarbonyl)-4-methyl-3-phenylisoxazol-5(2H)-one (4p). Yield = 31%; oil. ^{1}H NMR ($CDCl_3$-d_1) δ 1.04–1.09 (m, 2H, CH_2 cC_3H_5), 1.10–1.15 (m, 2H, CH_2 cC_3H_5), 1.86 (s, 3H, CH_3), 2.38–2.44 (m, 1H, CH cC_3H_5), 7.36–7.41 (m, 2H, Ar), 7.43–7.48 (m, 3H, Ar). ^{13}C NMR ($CDCl_3$-d_1) δ 7.30 (CH_3), 10.55 (CH_2), 12.71 (CH), 104.82 (C), 127.78 (C), 128.21 (CH), 128.35 (CH), 128.51 (CH), 130.44 (CH), 154.89 (C), 168.03 (C), 168.99 (C). ESI-MS calcd. for $C_{14}H_{13}NO_3$, 243.26; found: *m/z* 244.09 $[M+H]^+$. Anal. $C_{14}H_{13}NO_3$ (C, H, N).

2-(3-Methylbenzoyl)-3-phenylisoxazol-5(2H)-one (4q). Yield = 72%; oil. ^{1}H NMR ($CDCl_3$-d_1) δ 2.46 (s, 3H, m-CH_3-Ph), 6.54 (s, 1H, CH), 7.43–7.50 (m, 5H, Ar), 7.82–7.87 (m, 2H, Ar), 8.11–8.16 (m, 2H, Ar). ^{13}C NMR ($CDCl_3$-d_1) δ 21.24 (CH_3), 85.88 (CH), 126.76 (CH), 126.98 (C), 127.94 (CH), 129.04 (CH), 129.18 (C), 130.38 (CH), 131.23 (CH), 135.69 (CH), 139.06 (C), 160.47 (C), 164.26 (C), 165.70 (C). IR (υ) = 1600 cm^{-1} (CO amide), 1757 cm^{-1} (CO ester). ESI-MS calcd. for $C_{17}H_{13}NO_3$, 279.29; found: *m/z* 280.09 $[M+H]^+$. Anal. $C_{17}H_{13}NO_3$ (C, H, N).

2-(Cyclopropanecarbonyl)-3-phenylisoxazol-5(2H)-one (4r). Yield = 57%; oil. ^{1}H NMR ($CDCl_3$-d_1) δ 1.10–1.16 (m, 2H, CH_2 cC_3H_5), 1.23–1.28 (m, 2H, CH_2 cC_3H_5), 1.84–1.90 (m, 1H, CH cC_3H_5), 6.34 (s, 1H, CH), 7.42–7.47 (m, 3H, Ar), 7.74–7.79 (m, 2H, Ar). ^{13}C NMR ($CDCl_3$-d_1) δ 10.82 (CH_2), 12.71 (CH), 85.75 (CH), 126.55 (CH), 128.87 (CH), 129.27 (C), 130.26 (CH), 164.15 (C), 165.51 (C), 168.48 (C). ESI-MS calcd. for $C_{13}H_{11}NO_3$, 229.23; found: *m/z* 230.08 $[M+H]^+$. Anal. $C_{13}H_{11}NO_3$ (C, H, N).

2-(3-Methylbenzoyl)-3-(4-nitrophenyl)isoxazol-5(2H)-one (4s). Yield = 40%; mp = 177–180 °C dec. (EtOH). ^{1}H NMR (DMSO-d_6) δ 2.42 (s, 3H, m-CH_3-Ph), 7.13 (s, 1H, CH), 7.54 (t, 1H, Ar, $J = 7.6$ Hz), 7.64 (d, 1H, Ar, $J = 7.6$ Hz), 7.95–8.00 (m, 2H, Ar), 8.20 (d, 2H, Ar, $J = 8.8$ Hz), 8.36 (d, 2H, Ar, $J = 8.8$ Hz). ^{13}C NMR (DMSO-d_6) δ 21.27 (CH_3), 124.60 (CH), 125.76 (C), 126.91 (CH), 127.99 (CH), 128.28 (CH), 128.91 (CH), 130.18 (CH), 131.20 (C), 133.90 (CH), 136.50 (C), 138.35 (C), 148.54 (C), 160.45 (C), 167.84 (C). ESI-MS calcd. for $C_{17}H_{12}N_2O_5$, 324.29; found: *m/z* 325.08 $[M+H]^+$. Anal. $C_{17}H_{12}N_2O_5$ (C, H, N).

2-(Cyclopropanecarbonyl)-3-(4-nitrophenyl)isoxazol-5(2H)-one (4t). Yield = 23%; mp = 160–163 °C (EtOH). ^{1}H NMR ($CDCl_3$-d_1) δ 1.16–1.21 (m, 2H, CH_2 cC_3H_5), 1.27–1.32 (m, 2H, CH_2 cC_3H_5), 1.87–1.94 (m, 1H, CH cC_3H_5), 6.43 (s, 1H, CH), 7.96 (d, 2H, Ar, $J = 8.8$ Hz), 8.31 (d, 2H, Ar, $J = 8.8$ Hz). ^{13}C NMR ($CDCl_3$-d_1) δ 10.55 (CH_2), 12.71 (CH), 86.27 (CH), 121.42 (C), 124.67 (CH), 127.37 (CH), 135.22 (C), 148.74 (C), 162.53 (C), 168.75 (C). ESI-MS calcd. for $C_{13}H_{10}N_2O_5$, 274.23; found: *m/z* 275.06 $[M+H]^+$. Anal. $C_{13}H_{10}N_2O_5$ (C, H, N).

General procedure for compounds (4i, 4l)

To a suspension of 4-(pivaloyoxy)benzoic acid[45] or 4-(pivalamido)-benzoic acid[46] (0.32 mmol) in 1 ml of anhydrous toluene, 0.64 mmol of $SOCl_2$, and a catalytic amount of DMF (0.05 mmol) were added. The mixture was stirred at reflux for 2 h. The solvent was concentrated *in vacuo* and the crude compound was used without purification and added to a previously prepared solution composed of 0.29 mmol of intermediate **1a**[41] and 0.64 mmol of sodium hydride in 5 ml of anhydrous THF. The mixture was stirred at room temperature overnight. After evaporation of the solvent, the product was purified by column chromatography using toluene/ethyl acetate 9:1 for **4i** and hexane/acetone 4:1 for **4l** as eluents.

N-(4-(3-methyl-5-oxo-4-phenyl-2,5-dihydroisoxazole-2-carbonyl)-phenyl)pivalamide (4i). Yield = 10%; mp = 132–134 °C (EtOH). ^{1}H NMR ($CDCl_3$-d_1) δ 1.37 (s, 9H, $C(CH_3)_3$), 2.82 (s, 3H, CH_3), 7.41–7.46 (m, 1H, Ar), 7.49–7.55 (m, 4H, Ar), 7.73 (d, 2H, Ar, $J = 8.4$ Hz), 7.99 (d, 2H, Ar, $J = 8.8$ Hz). ^{13}C NMR ($CDCl_3$-d_1) δ 15.11 (CH_3), 27.56 (CH_3), 39.95 (C), 118.86 (CH), 126.01 (C), 127.54 (C), 127.66 (CH), 128.47 (CH), 128.82 (CH), 129.05 (CH), 131.65 (CH), 142.83 (C), 154.74 (C), 162.65 (C), 166.04 (C), 176.92 (C). ESI-MS calcd. for $C_{22}H_{22}N_2O_4$, 378.42; found: *m/z* 379.16 $[M+H]^+$. Anal. $C_{22}H_{22}N_2O_4$ (C, H, N).

4-(3-Methyl-5-oxo-4-phenyl-2,5-dihydroisoxazole-2-carbonyl)phenyl pivalate (4l). Yield = 41%; mp = 130–132 °C (EtOH). ^{1}H NMR ($CDCl_3$-d_1) δ 1.37 (s, 9H, $C(CH_3)_3$), 2.80 (s, 3H, CH_3), 7.22 (d, 2H, Ar, $J = 8.8$ Hz), 7.35–7.40 (m, 1H, Ar), 7.45–7.50 (m, 4H, Ar), 7.99 (d, 2H, Ar, $J = 8.8$ Hz). ^{13}C NMR ($CDCl_3$-d_1) δ 15.07 (CH_3), 27.07 (CH_3), 39.26 (C), 108.25 (C), 121.70 (CH), 127.56 (C), 128.16 (CH), 128.53 (CH), 128.83 (CH), 129.04 (CH), 131.70 (CH), 154.55 (C), 155.05 (C), 162.54 (C), 165.80 (C), 176.34 (C). IR (υ) = 1678 cm^{-1} (CO amide), 1753 cm^{-1} (CO ester), 1768 cm^{-1} (CO ester). ESI-MS calcd. for $C_{22}H_{21}NO_5$, 379.41; found: *m/z* 380.15 $[M+H]^+$. Anal. $C_{22}H_{21}NO_5$ (C, H, N).

General procedure for compounds (4m, 4u)

To a solution of intermediate **1b**[42] or **1f**[47] (0.32 mmol) in 2 ml of t-BuOH, 0.35 mmol of K_2CO_3 and 0.64 mmol of *m*-toluoyl chloride were added. The mixture was stirred at reflux for 3 h. The solvent was concentrated *in vacuo*, diluted with ice-cold water (10 ml), and extracted with DCM (3 × 15 ml). The organic phase was dried over sodium sulphate and the solvent was evaporated *in vacuo* to afford the final compounds **4m,u**, which were purified by column chromatography using cyclohexane/ethyl acetate in different ratio: 5:1 for **4m** and 1:1 for **4u** as eluent.

2-(3-Methylbenzoyl)-3,4-diphenylisoxazol-5(2H)-one (4m). Yield = 14%; mp = 160–163 °C (EtOH). ^{1}H NMR ($CDCl_3$-d_1) δ 2.42 (s, 3H, m-*CH*$_3$-Ph), 7.26–7.32 (m, 5H, Ar), 7.37–7.48 (m, 7H, Ar), 7.72–7.77 (m, 2H, Ar). ^{13}C NMR ($CDCl_3$-d_1) δ 21.40 (CH_3), 101.40 (C), 127.48 (CH), 128.31 (CH), 128.46 (CH), 128.53 (CH), 128.83 (CH), 130.74 (CH), 132.49 (C), 132.63 (C), 134.21 (C), 134.52 (CH), 138.50 (C), 142.65 (C), 157.66 (C), 165.80 (C). ESI-MS calcd. for $C_{23}H_{17}NO_3$, 355.39; found: *m/z* 356.12 $[M+H]^+$. Anal. $C_{23}H_{17}NO_3$ (C, H, N).

N-(4-(2-(3-methylbenzoyl)-5-oxo-2,5-dihydroisoxazol-3-yl)phenyl)acetamide (4u). Yield = 21%; oil. ^{1}H NMR ($CDCl_3$-d_1) δ 2.20 (s, 3H, CH_3CO), 2.45 (s, 3H, m-*CH*$_3$-Ph), 6.50 (s, 1H, CH), 7.42 (t, 1H, Ar, *J* = 7.8 Hz), 7.50 (d, 1H, Ar, *J* = 7.6 Hz), 7.56 (exch br s, 1H, NH), 7.62 (d, 2H, Ar, *J* = 8.0 Hz), 7.76 (d, 2H, Ar, *J* = 8.4 Hz), 7.98–8.13 (m, 2H, Ar). ^{13}C NMR ($CDCl_3$-d_1) δ 21.30 (CH_3), 24.81 (CH_3), 85.70 (C), 119.72 (CH), 127.45 (CH), 127.93 (CH), 128.88 (CH), 129.65 (C), 131.17 (CH), 134.11 (C), 135.75 (CH), 138.99 (C), 139.73 (C), 156.05 (C), 157.65 (C), 167.14 (C), 168.90 (C). ESI-MS calcd. for $C_{19}H_{16}N_2O_4$, 336.34; found: *m/z* 337.11 $[M+H]^+$. Anal. $C_{19}H_{16}N_2O_4$ (C, H, N).

General procedure for compounds (5e, 5f)

To a cooled (0 °C) suspension of **5d**[48] (0.68 mmol) in anhydrous CH_2Cl_2 (2 ml), Et_3N (1.36 mmol) and 2.04 mmol of appropriate acyl chloride were added. The mixture was stirred at 0 °C for 2 h and then at room temperature for an additional 2 h. The solvent was evaporated, cold water was added and the mixture was neutralised with 0.5 N NaOH. The reaction mixture was extracted with CH_2Cl_2 (3 × 15 ml), the solvent was dried over sodium sulphate, evaporated *in vacuo*, and compounds **5e** and **5f** were purified by column chromatography using dichloromethane/methanol (9:1 for **5e**; 99:1 for **5f**) as eluents.

Ethyl 2-(4-acetamidophenyl)-3-oxobutanoate (5e). Yield = 67%; mp = 112–113 °C (EtOH). ^{1}H NMR ($CDCl_3$-d_1) showed a 3:1 mixture of aldo-enol tautomers: δ 1.24 (t, 3H, CH_2*CH*$_3$, *J* = 7.0 Hz), 1.61 (t, 1H, CH_2*CH*$_3$, *J* = 7.0 Hz), 1.81 (s, 1H, $COCH_3$), 2.12 (s, 3H, $COCH_3$), 2.15 (s, 4H, $NHCOCH_3$), 4.16 (q, 2.7H, *CH*$_2$$CH_3$, *J* = 7.2 Hz), 4.65 (s,1H, CH), 7.06 (d, 0.7H, Ar, *J* = 8.0 Hz), 7.23 (d, 2H, Ar, *J* = 8.4 Hz), 7.48 (d, 2.7H, Ar, *J* = 8.0 Hz), 7.92 (exch br s, 1.3H, NH), 13.07 (exch br s, 0.3H, OH). ESI-MS calcd. for $C_{14}H_{17}NO_4$, 263.29; found: *m/z* 264.12 $[M+H]^+$. Anal. $C_{14}H_{17}NO_4$ (C, H, N).

Ethyl 2-(4-(ciclopropanecarboxamido)phenyl)-3-oxobutanoate (5f). Yield = 78%; oil. ^{1}H NMR ($CDCl_3$-d_1) showed the only aldo tautomer: δ 0.72–0.77 (m, 2H, CH_2 cC_3H_5), 0.80–0.85 (m, 2H, CH_2 cC_3H_5), 1.20 (t, 3H, CH_2*CH*$_3$, *J* = 7.2 Hz), 1.39–1.46 (m, 1H, CH cC_3H_5), 2.35 (s, 3H, $COCH_3$), 4.17 (q, 2H, *CH*$_2$$CH_3$, *J* = 7.2 Hz), 4.63 (s, 1H, CH), 7.19 (d, 2H, Ar, *J* = 8.4 Hz), 7.46 (d, 2H, Ar, *J* = 7.6 Hz), 7.52 (exch br s, 1H, NH). ESI-MS calcd. for $C_{16}H_{19}NO_4$, 289.33; found: *m/z* 290.13 $[M+H]^+$. Anal. $C_{16}H_{19}NO_4$ (C, H, N).

General procedure for compounds (6a–e)

A 3.00 mmol of appropriate intermediate **5a–c**[48–50] and **5e,f** was dissolved in 1.3 ml of water and heated at 80 °C. To this solution, 3.3 mmol of hydroxylamine hydrochloride in 6.5 ml of methanol was added. The mixture was stirred at reflux for 5 h. After evaporation of the solvent, the residue was mixed with ice-cold water (20 ml). Compounds **6a,c** were recovered by extraction with ethyl acetate (3 × 15 ml), while compounds **6b,d,e** were recovered by vacuum filtration. The final compounds **6b,d** were purified by crystallisation with ethanol, while the compounds **6a,c,e** were purified by column chromatography using dichoromethane/methanol 9:1 as eluent.

3-Methyl-4-(p-tolyl)isoxazol-5(2H)-one (6a). Yield = 35%; oil. ^{1}H NMR ($CDCl_3$-d_1) δ 2.17 (s, 3H, *CH*$_3$Ph), 2.28 (s, 3H, CH_3), 7.09 (d, 2H, Ar, *J* = 6.0 Hz), 7.28 (d, 2H, Ar, *J* = 6.0 Hz), 9.03 (exch br s, 1H, NH). ESI-MS calcd. for $C_{11}H_{11}NO_2$, 189.21; found: *m/z* 190.08 $[M+H]^+$. Anal. $C_{11}H_{11}NO_2$ (C, H, N).

4-(3-Methyl-5-oxo-2,5-dihydroisoxazol-4-yl)benzonitrile (6b). Yield = 72%; mp = 114–116 °C (EtOH). ^{1}H NMR ($CDCl_3$-d_1) δ 2.43 (s, 3H, CH_3), 7.70 (s, 4H, Ar). IR (υ) = 2270 cm^{-1} (CN). ESI-MS calcd. for $C_{11}H_8N_2O_2$, 200.19; found: *m/z* 201.06 $[M+H]^+$. Anal. $C_{11}H_8N_2O_2$ (C, H, N).

3-Methyl-4-(4-nitrophenyl)isoxazol-5(2H)-one (6c). Yield = 27%; mp = 208–209 °C (EtOH). ^{1}H NMR (DMSO-d_6) δ 2.19 (s, 3H, CH_3), 7.83 (d, 2H, Ar, *J* = 9.2 Hz), 7.94 (d, 2H, Ar, *J* = 8.4 Hz). ESI-MS calcd. for $C_{10}H_8N_2O_4$, 220.18; found: *m/z* 221.05 $[M+H]^+$. Anal. $C_{10}H_8N_2O_4$ (C, H, N).

N-(4-(3-methyl-5-oxo-2,5-dihydroisoxazol-4-yl)phenyl)acetamide (6d). Yield = 75%; mp = 210–212 °C (EtOH). ^{1}H NMR (DMSO-d_6) δ 2.01 (s, 3H, $NHCOCH_3$), 2.27 (s, 3H, CH_3), 7.43 (d, 2H, Ar, *J* = 8.0 Hz); 7.56 (d, 2H, Ar, *J* = 8.0 Hz), 9.92 (exch br s, 1H, *NH*$COCH_3$), 12.54 (exch br s, 1H, NH). ESI-MS calcd. for $C_{12}H_{12}N_2O_3$, 232.24; found: *m/z* 233.09 $[M+H]^+$. Anal. $C_{12}H_{12}N_2O_3$ (C, H, N).

N-(4-(3-methyl-5-oxo-2,5-dihydroisoxazol-4-yl)phenyl)cyclopropanecarboxamide (6e). Yield = 58%; mp = 208–210 °C (EtOH). ^{1}H NMR (DMSO-d_6) δ 0.70–0.75 (m, 4H, 2 × CH_2 cC_3H_5), 1.70–1.75 (m,1H, CH), 2.12 (s, 3H, CH_3), 7.40 (d, 2H, Ar, *J* = 8.4 Hz), 7.47 (d, 2H, Ar, *J* = 8.4 Hz), 9.97 (exch br s, 1H, *NH*CO cC_3H_5), 12.50 (exch br s, 1H, NH). ESI-MS calcd. for $C_{14}H_{14}N_2O_3$, 258.27; found: *m/z* 259.10 $[M+H]^+$. Anal. $C_{14}H_{14}N_2O_3$ (C, H, N).

General procedure for compounds (7a–e, 8a,b,d,e)

Compounds **7a–e** and **8a,b,d,e** were obtained following the same procedure performed for compounds **4a–h, 4n–t** but starting from precursors **6a–e**. The solvent was concentrated *in vacuo* to obtain the final compounds which were purified by column chromatography using petroleum ether/ethyl acetate 10:1 for **7a**/**8a**, hexane/ethyl acetate (5:1 for **7b/8b**; 5:2 for **7c**), dichloromethane/methanol (98:2 for **7d/8d**; 99:1 for **7e/8e**) as eluents.

3-Methyl-2-(3-methylbenzoyl)-4-(p-tolyl)isoxazol-5(2H)-one (7a). Yield = 60%; oil. ^{1}H NMR ($CDCl_3$-d_1) δ 2.39 (s, 3H, *p*-*CH*$_3$Ph), 2.43 (s, 3H, *m*-*CH*$_3$Ph), 2.79 (s, 3H, CH_3), 7.27 (d, 2H, Ar, *J* = 8.4 Hz), 7.37–7.42 (m, 4H, Ar), 7.70 (d, 2H, Ar, *J* = 6.8 Hz). ^{13}C NMR ($CDCl_3$-d_1) δ 15.05 (CH_3), 21.33 (CH_3), 108.19 (C), 124.63 (C), 127.03 (CH), 128.30 (CH), 128.89 (CH), 129.52 (CH), 130.24 (CH), 131.27 (C),

134.00 (CH), 138.28 (C), 138.48 (C), 154.09 (C), 163.82 (C), 166.07 (C). ESI-MS calcd. for $C_{19}H_{17}NO_3$, 307.34; found: *m/z* 308.12 $[M+H]^+$. Anal. $C_{19}H_{17}NO_3$ (C, H, N).

4-(3-Methyl-2-(3-methylbenzoyl)-5-oxo-2,5-dihydroisoxazol-4-yl)benzonitrile (7b). Yield = 26%; mp = 108–110 °C (EtOH). ^{1}H NMR ($CDCl_3$-d_1) δ 2.44 (s, 3H, CH_3Ph), 2.84 (s, 3H, CH_3), 7.38–7.48 (m, 2H, Ar), 7.65 (d, 2H, Ar, J = 8.4 Hz), 7.71 (d, 2H, Ar, J = 8.0 Hz), 7.76 (d, 2H, Ar, J = 8.4 Hz). ^{13}C NMR ($CDCl_3$-d_1) δ 15.19 (CH_3), 21.37 (CH_3), 29.70 (C), 106.24 (C), 112.03 (C), 118.41 (C), 127.13 (CH), 128.43 (CH), 129.43 (CH), 130.34 (CH), 130.72 (C), 132.52 (CH), 132.74 (C), 134.45 (CH), 138.49 (C), 155.56 (C), 163.79 (C), 165.15 (C). ESI-MS calcd. for $C_{19}H_{14}N_2O_3$, 318.33; found: *m/z* 319.10 $[M+H]^+$. Anal. $C_{19}H_{14}N_2O_3$ (C, H, N).

3-Methyl-2-(3-methylbenzoyl)-4-(4-nitrophenyl)isoxazol-5(2H)-one (7c). Yield = 6%; mp = 152–154 °C (EtOH). ^{1}H NMR ($CDCl_3$-d_1) δ 2.45 (s, 3H, CH_3Ph), 2.86 (s, 3H, CH_3), 7.39–7.46 (m, 2H, Ar), 7.72 (d, 4H, Ar, J = 8.8 Hz), 8.32 (d, 2H, Ar, J = 8.8 Hz). ^{13}C NMR ($CDCl_3$-d_1) δ 13.21 (CH_3), 21.32 (CH_3), 29.70 (C), 124.02 (CH), 127.16 (CH), 128.45 (CH), 129.56 (CH), 130.36 (CH), 130.65 (C), 134.51 (CH), 134.69 (C), 138.52 (C), 147.37 (C), 155.78 (C), 163.80 (C). ESI-MS calcd. for $C_{18}H_{14}N_2O_5$, 338.31; found: *m/z* 339.09 $[M+H]^+$. Anal. $C_{18}H_{14}N_2O_5$ (C, H, N).

N-(4-(3-methyl-2-(3-methylbenzoyl)-5-oxo-2,5-dihydroisoxazol-4-yl)phenyl)acetamide (7d). Yield = 37%; mp = 159–160 °C (EtOH). ^{1}H NMR ($CDCl_3$-d_1) δ 2.14 (s, 3H, NHCOCH_3), 2.41 (s, 3H, CH_3Ph), 2.75 (s, 3H, CH_3), 7.34–7.40 (m, 4H, Ar), 7.58 (d, 2H, Ar, J = 8.4 Hz), 7.67 (s, 2H, Ar), 7.97 (exch br s, 1H, NH). ^{13}C NMR ($CDCl_3$-d_1) δ 15.06 (CH_3), 21.35 (CH_3), 24.53 (CH_3), 120.11 (CH), 123.11 (C), 126.99 (CH), 128.33 (CH), 128.94 (CH), 129.61 (CH), 130.23 (CH), 131.11 (C), 131.27 (CH), 134.12 (CH), 138.29 (C), 154.40 (C), 163.79 (C), 166.26 (C), 168.87 (C). ESI-MS calcd. for $C_{20}H_{18}N_2O_4$, 350.37; found: *m/z* 351.13 $[M+H]^+$. Anal. $C_{20}H_{18}N_2O_4$ (C, H, N).

N-(4-(3-methyl-2-(3-methylbenzoyl)-5-oxo-2,5-dihydroisoxazol-4-yl) phenyl)ciclopropanecarboxamide (7e). Yield = 6%; mp = 120–123 °C (EtOH). ^{1}H NMR ($CDCl_3$-d_1) δ 0.84–0.89 (m, 2H, CH_2 cC_3H_5), 1.07–1.12 (m, 2H, CH_2 cC_3H_5), 1.24 (s, 1H, CH), 2.43 (s, 3H, CH_3Ph), 2.79 (s, 3H, CH_3), 7.36–7.41 (m, 2H, Ar), 7.46 (d, 2H, Ar, J = 8.4 Hz), 7.61 (d, 2H, Ar, J = 8.4 Hz), 7.70 (d, 2H, Ar, J = 7.2 Hz). ^{13}C NMR ($CDCl_3$-d_1) δ 8.24 (CH_2), 15.13 (CH_3), 15.88 (CH), 21.41 (CH_3), 107.20 (C), 119.79 (CH), 127.03 (CH), 128.33 (CH), 129.68 (CH), 130.25 (CH), 130.30 (C), 134.09 (CH), 134.10 (C), 137.70 (C), 138.33 (C), 139.50 (C), 157.61 (C), 163.83 (C), 180.70 (C). ESI-MS calcd. for $C_{22}H_{20}N_2O_4$, 376.41; found: *m/z* 377.15 $[M+H]^+$. Anal. $C_{22}H_{20}N_2O_4$ (C, H, N).

3-Methyl-4-(p-tolyl)isoxazol-5-yl 3-methylbenzoate (8a). Yield = 12%; oil. ^{1}H NMR ($CDCl_3$-d_1) δ 2.33 (s, 3H, *p*-CH_3Ph), 2.38 (s, 3H, CH_3), 2.41 (s, 3H, *m*-CH_3Ph), 7.18 (d, 2H, Ar, J = 8.0 Hz), 7.24 (d, 2H, Ar, J = 8.4 Hz), 7.38 (t, 1H, Ar, J = 8.0 Hz), 7.47 (d, 1H, Ar, J = 7.2 Hz), 7.93 (s, 2H, Ar). ^{13}C NMR ($CDCl_3$-d_1) δ 12.21 (CH_3), 21.23 (CH_3), 100.50 (C), 127.97 (CH), 128.10 (CH), 128.75 (CH), 129.63 (CH), 130.10 (C), 131.26 (CH), 133.30 (C), 135.57 (CH), 138.84 (C), 154.20 (C), 158.90 (C), 165.20 (C). ESI-MS calcd. for $C_{19}H_{17}NO_3$, 307.34; found: *m/z* 308.12 $[M+H]^+$. Anal. $C_{19}H_{17}NO_3$ (C, H, N).

4-(4-Cyanophenyl)-3-methylisoxazol-5-yl 3-methylbenzoate (8b). Yield = 20%; mp = 98–100 °C (EtOH). ^{1}H NMR ($CDCl_3$-d_1) δ 2.41 (s, 3H, CH_3), 2.43 (s, 3H, CH_3Ph), 7.43 (t, 1H, Ar, J = 8.0 Hz), 7.47 (d, 2H, Ar, J = 8.4 Hz), 7.51 (d, 1H, Ar, J = 7.6 Hz), 7.67 (d, 2H, Ar, J = 8.4 Hz), 7.92 (s, 2H, Ar). ^{13}C NMR ($CDCl_3$-d_1) δ 12.31 (CH_3), 21.25 (CH_3), 29.70 (C), 111.68 (C), 118.37 (C), 126.33 (C), 128.02 (CH), 128.61 (CH), 128.95 (CH), 131.30 (CH), 132.75 (CH), 133.27 (C), 136.04 (CH), 139.11 (C), 160.61 (C), 161.90 (C). ESI-MS calcd. for $C_{19}H_{14}N_2O_3$, 318.33; found: *m/z* 319.10 $[M+H]^+$. Anal. $C_{19}H_{14}N_2O_3$ (C, H, N).

4-(4-Acetamidophenyl)-3-methylisoxazol-5-yl3-methylbenzoate (8d). Yield = 10%; mp = 57–60 °C (EtOH). ^{1}H NMR ($CDCl_3$-d_1) δ 2.15 (s, 3H, NHCOCH_3), 2.36 (s, 3H, CH_3), 2.41 (s, 3H, CH_3Ph), 7.29 (d, 3H, Ar, J = 8.4 Hz), 7.38 (t, 1H, Ar, J = 8.0 Hz), 7.46 (exch br s, 1H, NH), 7.51 (d, 2H, Ar, J = 8.4 Hz), 7.91 (s, 2H, Ar). ^{13}C NMR ($CDCl_3$-d_1) δ 12.23 (CH_3), 21.24 (CH_3), 24.59 (CH_3), 29.69 (C), 120.11 (CH), 123.90 (C), 126.71 (C), 127.97 (CH), 128.83 (CH), 129.67 (CH), 131.26 (CH), 135.70 (CH), 137.61 (C), 138.91 (C), 161.21 (C), 162.31 (C), 168.39 (C). ESI-MS calcd. for $C_{20}H_{18}N_2O_4$, 350.37; found: *m/z* 351.13 $[M+H]^+$. Anal. $C_{20}H_{18}N_2O_4$ (C, H, N).

4-(4-(Ciclopropanecarboxamido)phenyl)-3-methylisoxazol-5-yl3-methylbenzoate (8e). Yield = 8%; mp = 80–82 °C (EtOH). ^{1}H NMR ($CDCl_3$-d_1) δ 0.80–0.90 (m, 4H, 2 × CH_2 cC_3H_5), 1.35–1.40 (m, 1H, CH), 2.37 (s, 3H, CH_3), 2.41 (s, 3H, CH_3Ph), 7.28 (d, 2H, Ar, J = 8.0 Hz), 7.38 (t, 1H, Ar, J = 7.6 Hz), 7.40 (exch br s,1H, NH), 7.47 (d, 1H, Ar, J = 7.6 Hz), 7.52 (d, 2H, Ar, J = 7.2 Hz), 7.92 (s, 2H, Ar). ^{13}C NMR ($CDCl_3$-d_1) δ 8.15 (CH_2), 12.24 (CH_3), 14.90 (CH), 21.25 (CH_3), 100.52 (C), 119.91 (CH), 127.97 (CH), 128.79 (CH), 128.85 (CH), 131.25 (CH), 132.05 (C), 135.68 (CH), 138.70 (C), 138.89 (C), 154.20 (C), 158.90 (C), 165.20 (C), 180.70 (C). ESI-MS calcd. for $C_{22}H_{20}N_2O_4$, 376.41; found: *m/z* 377.15 $[M+H]^+$. Anal. $C_{22}H_{20}N_2O_4$ (C, H, N).

General procedure for compounds (10a–c)

To suspension of the substrate **9**[51] (0.37 mmol) in *tert*-Butanol (3 ml), K_2CO_3 (0.41 mmol), and 0.74 mmol of the appropriate acyl chloride were added. The mixture was stirred at reflux for 3 h. After evaporation of the solvent, the residue was mixed with ice-cold water (20 ml) and extracted with ethyl acetate (3 × 15 ml). The organic phase was dried over sodium sulphate, and the solvent was evaporated *in vacuo* to afford the final compounds 1**0a–c**, which were purified by column chromatography using cyclohexane/ethyl acetate (5:1) as eluent.

1-Propionylbenzo[c]isoxazol-3(1H)-one (10a). Yield = 7%; oil. ^{1}H NMR ($CDCl_3$-d_1) δ 1.28 (t, 3H, CH_2CH_3, J = 7.4 Hz), 2.83 (q, 2H, CH_2CH_3, J = 7.2 Hz), 7.38 (t 1H, Ar, J = 7.6 Hz), 7.78 (t 1H, Ar, J = 7.6 Hz), 7.89 (d, 1H, Ar, J = 8.0 Hz), 8.11 (d, 1H, Ar, J = 8.4 Hz). ^{13}C NMR ($CDCl_3$-d_1) δ 9.72 (CH_3), 20.70 (CH_2), 120.35 (CH), 122.50 (C), 124.09 (CH), 130.31 (CH), 133.90 (CH), 142.44 (C), 166.02 (C), 172.05 (C). ESI-MS calcd. for $C_{10}H_9NO_3$, 191.18; found: *m/z* 192.06 $[M+H]^+$. Anal. $C_{10}H_9NO_3$ (C, H, N).

1-Pentanoylbenzo[c]isoxazol-3(1H)-one (10b). Yield = 12%; oil. ^{1}H NMR ($CDCl_3$-d_1) δ 0.87 (t, 3H, $CH_3CH_2CH_2CH_2CO$, J = 6.8 Hz), 1.53–1.58 (m, 2H, $CH_3CH_2CH_2CH_2CO$), 1.98–2.03 (m, 2H, $CH_3CH_2CH_2CH_2CO$), 3.63 (t, 2H, $CH_3CH_2CH_2CH_2CO$, J = 6.8 Hz), 7.22 (d, 1H, Ar, J = 8.4 Hz), 7.31 (t, 1H, Ar, J = 7.4 Hz), 7.68 (t, 1H, Ar, J = 7.6 Hz), 7.86 (d, 1H, Ar, J = 7.6 Hz). ^{13}C NMR ($CDCl_3$-d_1) δ 13.10 (CH_3), 22.15 (CH_2), 27.65 (CH_2), 28.21 (CH_2), 120.31 (CH), 122.49 (C), 124.00 (CH), 130.33 (CH), 133.90 (CH), 142.41 (C), 165.31 (C), 172.22 (C). ESI-MS calcd. for $C_{12}H_{13}NO_3$, 219.24; found: *m/z* 220.09 $[M+H]^+$. Anal. $C_{12}H_{13}NO_3$ (C, H, N).

1-(3-Methylbenzoyl)benzo[c]isoxazol-3(1H)-one (10c). Yield = 53%; mp = 116–119 °C (EtOH). ^{1}H NMR ($CDCl_3$-d_1) δ 2.44 (s, 3H, CH_3), 7.39–7.45 (m, 3H, Ar), 7.75–7.80 (m, 2H, Ar), 7.83 (t 1H, Ar, J = 8.4 Hz), 7.92 (d, 1H, Ar, J = 8.0 Hz), 8.22 (d, 1H, Ar, J = 8.4 Hz). ^{13}C NMR ($CDCl_3$-d_1) δ 21.40 (CH_3), 115.83 (CH), 117.51 (C), 125.60 (CH), 126.03 (CH), 126.87 (CH), 128.34 (CH), 130.12 (CH), 133.40 (C), 133.81 (CH), 136.54 (CH), 137.80 (C), 151.60 (C), 158.51 (C), 172.03 (C). ESI-MS calcd. for $C_{15}H_{11}NO_3$, 253.25; found: *m/z* 254.08 $[M+H]^+$. Anal. $C_{15}H_{11}NO_3$ (C, H, N).

HNE inhibition assay

Compounds were dissolved in 100% DMSO at 5 mM stock concentrations. The final concentration of DMSO in the reactions was 1%, and this level of DMSO had no effect on enzyme activity. The HNE inhibition assay was performed in black flat-bottom 96-well microtiter plates. Briefly, a buffer solution containing 200 mM Tris–HCl, pH 7.5, 0.01% bovine serum albumin, and 0.05% Tween-20 and 20 mU/mL of HNE (Calbiochem) was added to wells containing different concentrations of each compound. The reaction was initiated by addition of 25 μM elastase substrate (N-methylsuccinyl-Ala-Ala-Pro-Val-7-amino-4-methylcoumarin, Calbiochem) in a final reaction volume of 100 μl/well. Kinetic measurements were obtained every 30 s for 10 min at 25 °C using a Fluoroskan Ascent FL fluorescence microplate reader (Thermo Electron, MA) with excitation and emission wavelengths set at 355 and 460 nm, respectively. For all compounds tested, the concentration of inhibitor that caused 50% inhibition of the enzymatic reaction (IC_{50}) was calculated by plotting % inhibition versus logarithm of inhibitor concentration (at least six points). The data are presented as the mean values of at least three independent experiments with relative standard deviations of <15%.

Analysis of compound stability

Spontaneous hydrolysis of selected derivatives was evaluated at 25 °C in 0.05 M phosphate buffer, pH 7.3. Kinetics of hydrolysis were monitored by measuring changes in the absorbance spectra over time using a SpectraMax Plus microplate spectrophotometer (Molecular Devices, Sunnyvale, CA). Absorbance (A_t) at the characteristic absorption maxima of each compound was measured at the indicated times until no further absorbance decreases occurred (A_∞)[52]. Using these measurements, we created semilogarithmic plots of $\log(A_t–A_\infty)$ versus time, and k' values were determined from the slopes of these plots. Half-conversion times were calculated using $t_{1/2} = 0.693/k'$, as described previously[36,37].

Molecular modelling procedures

The programs used for the energy minimisation, MD, and docking were the simulation protocols Minimisation, Standard Dynamics Cascade, Analyse Trajectory, and CDocker implemented in Accelrys Discovery Studio 2.1[53]. The Force Field used for all simulations was CHARMm[54].

The following parameters were used for MD simulations, both in vacuum and in implicit solvent (the latter was simulated by using distance dependent dielectric constant set to 4r): time step = 1 fs, equilibration time = 100 ps, production time = 1000 ps (5000 ps for the inhibitor-HNE assembly), T = 300 and 600 K. Ten snapshot conformations with evenly spaced intervals were extracted from each MD trajectory and subsequently minimised (using the steepest descent and conjugate gradient algorithms) in order to obtain the starting geometries for the subsequent quantum chemical calculations (QC) and MD simulations with the receptor.

GAUSSIAN09 (REV. C01)[55] was used for quantum chemical calculations (QC) on **7d** and **8d** by using the B3LYP[56,57] and B97D[58] functionals. The basis set was 6-31 + G(d,p)[59], and the Berny algorithm was used[60]. Reliability of the stationary points was assessed by evaluation of the vibrational frequencies. For each inhibitor, different conformational isomers, chosen from amongst the low lying energy conformers (as found in MD simulations and subsequent geometry optimisation) were considered.

Molecular plots were produced by the program Discovery Studio Visualiser (v 4.5)[61].

Results and discussion

Chemistry

It is well-known that the isoxazolone nucleus exhibits three tautomers[43,62,63], as illustrated below. The NH form seems to be the most representative, especially in polar solvents[62,64–66]. However, it is possible to find examples of alkylation and acylation products in the literature, as shown by the NH and the OH forms[67]. Taking into account this information, we performed the synthesis of our final compounds, as shown in Schemes 1–3, and the structures were confirmed on the basis of analytical and spectral data.

Scheme 1 depicts the synthetic pathway followed to obtain the final 2-N-substituted isoxazolones of type **2**, **3**, and **4**, which have different groups at positions 3 and 4. The previously described key intermediate isoxazol-5-(2H)-ones of type **1** were treated under various conditions to obtain the final compounds **2**, **3**, and **4**. The alkylation of **1a**[41] with 3-methylbenzyl chloride and K_2CO_3 in anhydrous acetonitrile at reflux resulted in compound **2**. On the other hand, treatment of compounds **1a–f** (**1a**[41], **1b**[42], **1c,d**[43], **1e**[44], and **1f**[47]) with the appropriate acyl/aroyl chloride and NaH in anhydrous THF at room temperature (compounds **4a–l,n–t**) or with m-toluyl chloride, and K_2CO_3 in t-ButOH at 80 °C (compounds **4m,u**) resulted in the corresponding 2-NCO derivatives of type **4**. Likewise, we synthesised the sulfonamide derivatives **3a–c** by treatment of intermediate **1a**[41] with the appropriate commercially available phenyl sulfonyl chloride in pyridine at room temperature. All of these reactions led to a single derivative originating from the NH form of the isoxazolone nucleus, in agreement with previous data reported in literature.

Scheme 2 shows the synthetic procedures used to obtain the final compounds of type **7** and **8**, which have a 4-substituted phenyl at position 4. β-Ketoesters **5a–d** (**5a**[49], **5b,d**[48], and **5c**[50]) were synthesised as described previously[48–50], while compounds **5e,f** were obtained by acylation of **5d**[48] with the appropriate acyl chloride and Et_3N in dichloromethane. These compounds served as the starting material for synthesis of the key intermediates of type **6** with an isoxazolone nucleus. Cyclisation of **5a–c,e,f** with hydroxylamine hydrochloride in a mixture MeOH/H_2O 1:1 at reflux resulted in the intermediates **6a–e** which, in turn, were treated with m-toluoyl chloride under the same conditions reported in Scheme 1. Unexpectedly this last step resulted the pair of isomers of type **7** and **8** (NCO/OCO ratio 3:1), with the only exception being the nitro derivative **7c**, which was obtained only in the N-CO form.

Assignment of the isomer structures was first performed using the ^{1}H NMR chemical shift value of the methyl at position 3. Compounds **4a–l** (Scheme 1) had shifts of 2.8 ppm, which is characteristic of NCO derivatives. Likewise, we attributed the NCO-structure to compounds with a 2.8 ppm shift for 3-CH_3 (**7a–e**) and the OCO-structure to compounds with a 2.4 ppm shift (**8a,b,d,e**)

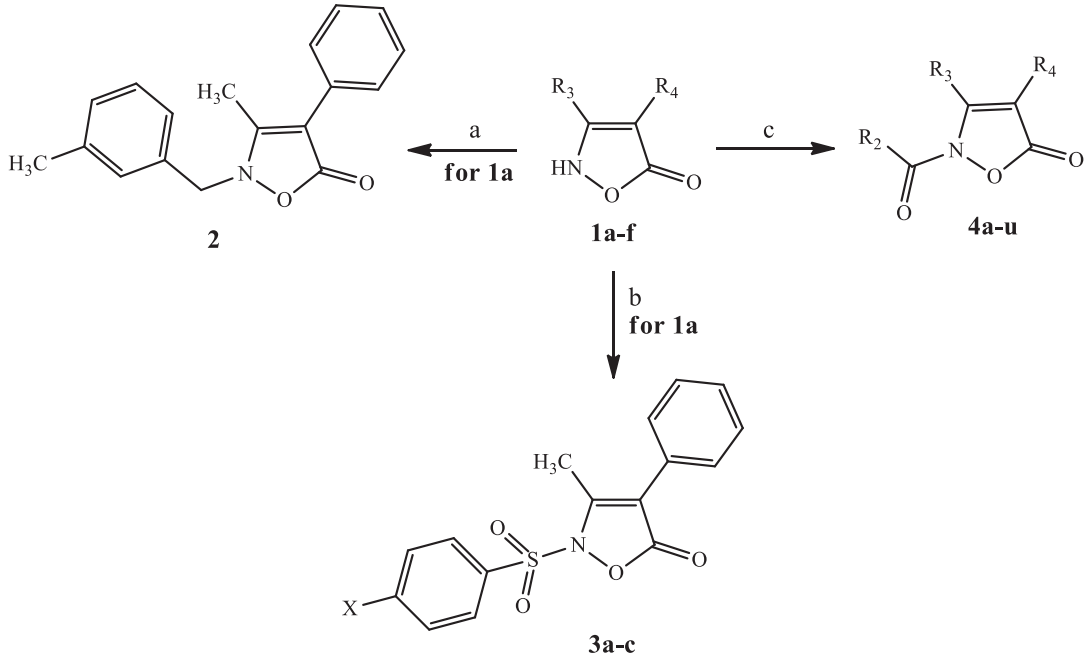

1	R_3	R_4
a	CH_3	Ph
b	Ph	Ph
c	Ph	CH_3
d	Ph	H
e	4-NO_2-Ph	H
f	4-$NHCOCH_3$-Ph	H

3	X
a	OH
b	$OCOC(CH_3)_3$
c	$NHCOC(CH_3)_3$

4	R_2	R_3	R_4
a	m-CH_3-Ph	CH_3	Ph
b	cC_3H_5	CH_3	Ph
c	p-CH_3-Ph	CH_3	Ph
d	o-CH_3-Ph	CH_3	Ph
e	m-CF_3-Ph	CH_3	Ph
f	m-SO_2CH_3-Ph	CH_3	Ph
g	m-CN-Ph	CH_3	Ph
h	p-CN-Ph	CH_3	Ph
i	p-$NHCOC(CH_3)_3$-Ph	CH_3	Ph
l	p-$OCOC(CH_3)_3$-Ph	CH_3	Ph
m	m-CH_3-Ph	Ph	Ph
n	cC_3H_5	Ph	Ph
o	m-CH_3-Ph	Ph	CH_3
p	cC_3H_5	Ph	CH_3
q	m-CH_3-Ph	Ph	H
r	cC_3H_5	Ph	H
s	m-CH_3-Ph	4-NO_2-Ph	H
t	cC_3H_5	4-NO_2-Ph	H
u	m-CH_3-Ph	4-$NHCOCH_3$-Ph	H

Scheme 1. Reagents and conditions: (a) 3-methylbenzyl chloride, K_2CO_3, anhydrous CH_3CN, 80 °C, 2 h; (b) 4-X-Ph-SO_2Cl, anhydrous pyridine, r.t., 4 h; (c) for **4a–l, n–t:** R_2-COCl, NaH, anhydrous THF, r.t., 24 h; for **4m,u**: m-toluoyl chloride, K_2CO_3, t-BuOH, 80 °C, 3 h.

(see Supporting Information). In order to verify our findings, we performed additional techniques, such as IR spectroscopy and 2 D NMR (^{1}H–^{13}C HSQC, ^{1}H–^{13}C HMBC, and ^{1}H–^{1}H NOESY).

In Scheme 3, we show the synthetic pathways used to obtain the benzoisoxazolone derivatives **10a–c**, which are an elaboration of the previous isoxazolone scaffold. The acylation of benzoisoxazolone intermediate **9**[51] with the appropriate acyl chloride and potassium carbonate in t-BuOH led to final compounds **10a–c**.

Biological evaluation and structure–activity relationship (SAR) analysis

All compounds were evaluated for their ability to inhibit HNE in comparison with Sivelestat, a reference HNE inhibitor, and the results presented in Tables 1–3. Previously[40], we examined the possibility of a two point of attack for Ser195, 2-NCO, and 5-CO, and docking studies confirmed that the endocyclic C = O at position 5 was involved in the catalysis process, whereas the amidic C = O group was important for anchoring to the sub-pocket of the binding site. We could expect a similar trend in this new series of isoxazolones.

Beginning analysis of the data with the 3-methyl-4-phenylisoxazol-5(2H)-one derivatives (compounds **4a–l**), the results reported in Table 1 suggest that, similar to our previous series[40], the best substituents at position N-2 are a m-methylbenzoyl or a cyclopropanecarbonyl fragment, which resulted in compounds **4a** and **4b** that were active in the nanomolar range (IC_{50} = 77 and 59 nM, respectively). Displacement of the methyl group from the meta to the para (**4c**) or ortho (**4d**) positions on the phenyl led to compounds with activity one order of magnitude lower than **4a**, which is different than our previous series[40], where moving the methyl

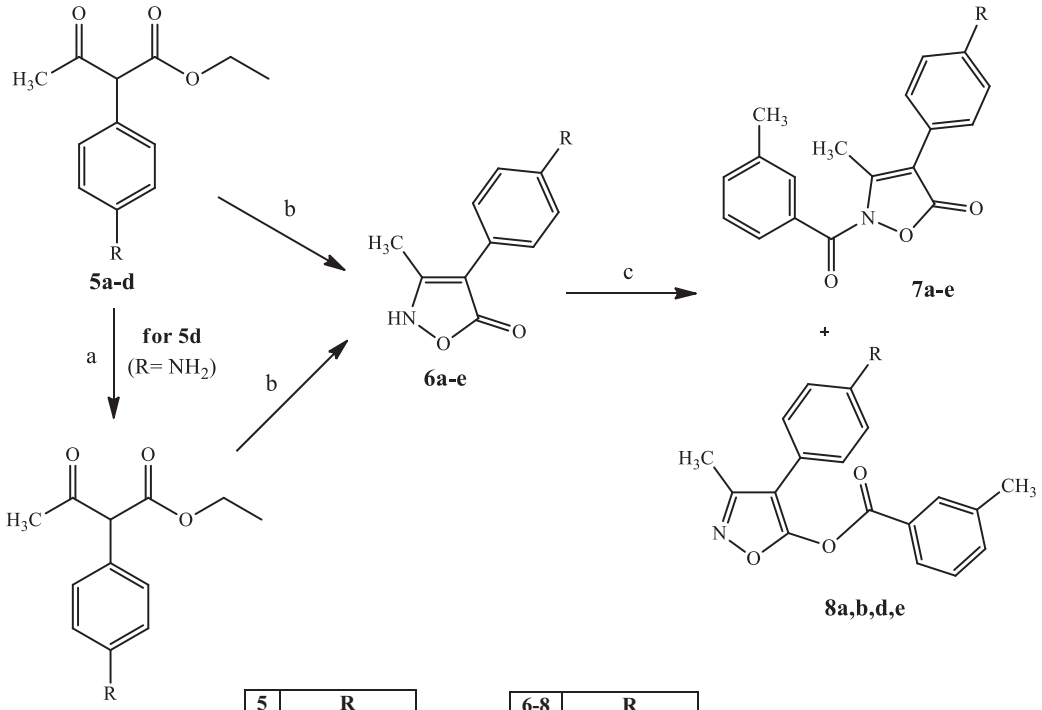

5	R
a	CH_3
b	CN
c	NO_2
d	NH_2
e	$NHCOCH_3$
f	$NHCOcC_3H_5$

6-8	R
a	CH_3
b	CN
c	NO_2
d	$NHCOCH_3$
e	$NHCOcC_3H_5$

Scheme 2. Reagents and conditions: (a) R-COCl, Et_3N, anhydrous CH_2Cl_2, 0 °C, 2 h, then r.t., 2 h; (b) $NH_2OH.HCl$, H_2O/MeOH 1:1, reflux, 5 h; (c) m-toluoyl chloride, NaH, anhydrous THF, r.t., 24 h.

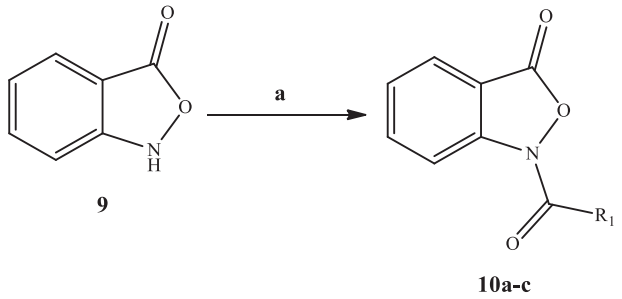

10	R_1
a	C_2H_5
b	C_4H_9
c	m-CH_3-Ph

Scheme 3. Reagents and conditions: (a) R_1-COCl, K_2CO_3, t-BuOH, 80 °C, 3 h.

to the para position had no effect on HNE inhibitory activity. Substitution of m-methyl with other groups, such as trifluoromethyl (**4e**), cyano (**4g,h**), or methylsulfonyl (**4f**), which are found in other potent HNE inhibitors, was not favourable for activity, and only compound **4e** exhibited activity in the submicromolar range (IC_{50} = 200 nM).

To evaluate the importance of the 2-CO amidic group in this series, we synthesised the alkyl derivative **2**, which was completely inactive, suggesting that the carbonyl group is important for HNE inhibitory activity and also probably involved in catalysis. The insertion of the 3-methyl-4-phenylisoxazol-5(2H)-one scaffold of the sulfonamide fragment of the drug Sivelestat at position 2 led to compound **3b**, which exhibited comparable activity to Sivelestat (IC_{50} = 59 nM, Table 1). In contrast, its pivalamide derivative (**3c**) was completely inactive, suggesting that the possible point of attack of Ser195 is the CO of the pivalate function, which is also present in Sivelestat. These data were also confirmed by the inactivity of the hydrolysed derivative **3a**. Moreover, we synthesised compounds **4l** and **4i** by substituting the SO_2 group at position 2 (**3b** and **3c**, respectively) with an amidic function. The amide **4l** had activity (IC_{50} = 0.48 μM) that was one order of magnitude higher than the corresponding sulfonamide **3b**, while the amide **4i** had a higher potency (IC_{50} = 8.5 μM) than its corresponding sulfonamide **3c**, which was completely inactive. These results suggest that the SO_2 group at position 2 of **3b** could also be important for anchoring the ligand to the sub-pocket of the binding site.

Keeping m-methylbenzoyl and ciclopropanecarbonyl at position N-2, we modified positions 3 and 4 of the isoxazolone (Table 1). Generally, we observed a collapse of activity. In particular, the 3,4-diphenylisoxazol-5(2H)-one derivatives (compounds **4m** and **4n**), the 4-methyl-3-phenylisoxazol-5(2H)-one derivatives (compounds **4o** and **4p**), and the 3-phenylisoxazol-5(2H)-one derivatives (compounds **4q,r** and **4u**) all had decreased activity (IC_{50} = 10–50 μM). The insertion in the para position of the phenyl ring at position 3 of compounds **4q,r** with substituents that in the previous series gave good results (such as a nitro group or acetamide function) led to completely inactive (compounds **4s,t**). Based on the results in Table 1, we can conclude that

Table 1. HNE inhibitory activity of isoxazolone derivatives **2**, **3a–c**, and **4a–u**.

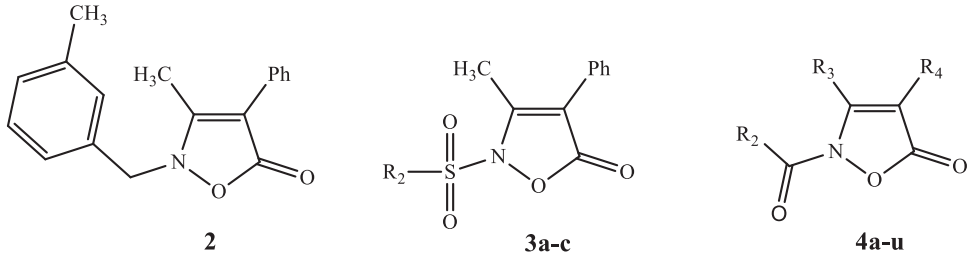

2 **3a-c** **4a-u**

Comp.	R_2	R_3	R_4	IC_{50} (μM)[a]
2	–	–	–	NA
3a	p-OH-Ph	–	–	NA.
3b	p-OCOC$(CH_3)_3$-Ph	–	–	0.059 ± 0.02
3c	p-NHCOC$(CH_3)_3$-Ph	–	–	NA
4a	m-CH_3-Ph	CH_3	Ph	0.077 ± 0.027
4b	cC_3H_5	CH_3	Ph	0.059 ± 0.018
4c	p-CH_3-Ph	CH_3	Ph	0.23 ± 0.034
4d	o-CH_3-Ph	CH_3	Ph	0.35 ± 0.036
4e	m-CF_3-Ph	CH_3	Ph	0.20 ± 0.027
4f	m-CH_3SO_2-Ph	CH_3	Ph	29.6 ± 7.2
4g	m-CN-Ph	CH_3	Ph	6.3 ± 1.4
4h	p-CN-Ph	CH_3	Ph	11.4 ± 1.9
4i	p-NHCOC$(CH_3)_3$-Ph	CH_3	Ph	8.5 ± 2.1
4l	p-OCOC$(CH_3)_3$-Ph	CH_3	Ph	0.48 ± 0.13
4m	m-CH_3-Ph	Ph	Ph	10.1 ± 1.3
4n	cC_3H_5	Ph	Ph	17.2 ± 2.3
4o	m-CH_3-Ph	Ph	CH_3	13.6 ± 2.4
4p	cC_3H_5	Ph	CH_3	1.1 ± 0.14
4q	m-CH_3-Ph	Ph	H	48.7 ± 3.3
4r	cC_3H_5	Ph	H	12.7 ± 2.7
4s	m-CH_3-Ph	4-NO_2-Ph	H	N.A.
4t	cC_3H_5	4-NO_2-Ph	H	N.A.
4u	m-CH_3-Ph	4-$NHCOCH_3$-Ph	H	28.6 ± 3.3
Sivelestat				0.044 ± 0.011

[a]IC_{50} values are presented as the mean ± SD of three independent experiments.
NA: no inhibitory activity was found at the highest concentration of compound tested (50 μM).

Table 2. HNE inhibitory activity of isoxazolone derivatives **7a–e** and **8a,b,d,e**.

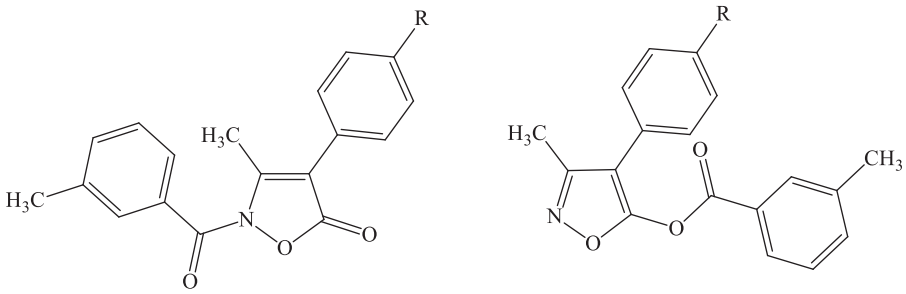

7a-e **8a,b,d,e**

Comp.	R	IC_{50} (μM)[a]
7a	CH_3	0.02 ± 0.009
8a	CH_3	10.2 ± 1.4
7b	CN	0.07 ± 0.02
8b	CN	0.42 ± 0.13
7c	NO_2	0.21 ± 0.04
7d	$NHCOCH_3$	0.05 ± 0.02
8d	$NHCOCH_3$	0.54 ± 0.11
7e	$NHCOcC_3H_5$	0.05 ± 0.02
8e	$NHCOcC_3H_5$	0.62 ± 0.21
Sivelestat		0.044 ± 0.011

[a]IC_{50} values are presented as the mean ± SD of three independent experiments.

position 4 can bear bulky groups, such as an aromatic ring, when there is a methyl group in position 3, probably to fit constraints of the lipophilic pocket. Moving the phenyl ring to position 3 is not tolerated, either when there is a methyl or a hydrogen present in position 4.

In Table 2, we report the activity of the pair of isomers of type **7** and **8**, the amidic and ester derivatives, respectively, which were obtained by introducing a substituent to the para position of the phenyl group at position 4. All N-benzoyl derivatives (**7a–e**), with the exception of the nitro compound **7c**,

Table 3. HNE inhibitory activity of benzoisoxazolone derivatives **10a–c**.

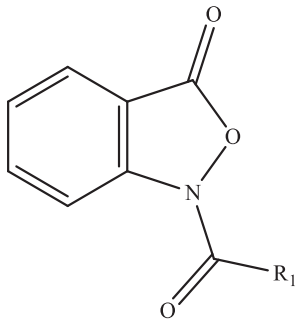

10a-c

Comp.	R_1	IC_{50} (μM)[a]
10a	C_2H_5	25.1 ± 3.6
10b	C_4H_9	NA
10c	m-CH_3-Ph	0.638 ± 0.121
Sivelestat		0.044 ± 0.011

[a]IC_{50} values are presented as the mean ± SD of three independent experiments.
NA: no inhibitory activity was found at the highest concentration of compound tested (50 μM).

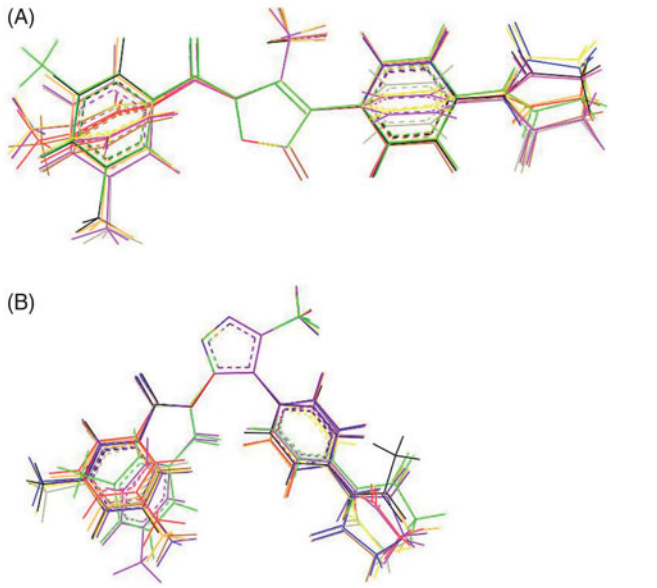

Figure 2. Panel (A): Superimposition of the minimised conformations of **7d** extracted from the MD trajectory ($T = 600$ K, $\varepsilon = 4r$). Panel (B): Superimposition of the minimised conformations of **8d** extracted from the MD trajectory ($T = 600$ K, $\varepsilon = 4r$).

exhibited good HNE inhibitory activity in the nanomolar range ($IC_{50} = 20$–70 nM). In addition, the activity seems to be independent of the electrophilic properties of the substituents (CH_3, NO_2, CN, NHCOR). The best compound of this series was the p-methyl derivative **7a**, which had an IC_{50} of 20 nM. The O-benzoyl derivatives **8b,d,e**, which were derived from tautomerism of the isoxazolone scaffold, surprisingly exhibited activity, although at one order of magnitude lower than the corresponding N-benzoyl type **7** derivatives (Table 2). Only the ester isomer of the potent **7a** had a significant loss in activity (**8a**, $IC_{50} = 10$ μM). The unexpected data related to esters **8a,b,d,e** could indicate a different interaction with the target, since the CO endocyclic implicated in the catalysis is missing, and the only carbonyl group presented in the molecule is an ester function at position 5. Further docking studies and kinetic experiments could help us to understand the interaction of these compounds with the HNE catalytic site and their mechanism of action.

Table 3 shows the HNE inhibitory activity of benzoisoxazolone derivatives **10a–c**, which are elaborations of the isoxazolone scaffold. In this case, only the m-methylbenzoyl derivative **10c** had reasonable activity, with an IC_{50} of 638 nM, while the other compounds were less active (**10a**) or inactive (**10b**).

Molecular modelling

Several attempts were made using different solvents in order to obtain crystals of **7d** and **8d**. However, it was not possible to obtain crystals suitable for X-ray diffraction (probably in part due to their quite low melting points). As a consequence, the starting 3D geometry of these molecules was obtained by using as building blocks the solid state structures of 3,5-dicyano-4-(4-methoxyphenyl) isoxazole (QAQPON refcode)[68] found in the Cambridge Structural Database (CSD; v 5.37)[69] and that of the isoxazolone derivative **2j** (3-ethyl-2–(3-methylbenzoyl)isoxazol-5(2H)-one)[40]. The 3D arrangement of **7d** and **8d** was then roughly improved by an energy minimisation procedure, followed by molecular dynamics simulations (details in the Supplementary Material).

Preliminary molecular dynamics (MD) simulations at 300 and 600 K were performed on **7d** and **8d** to evaluate their flexibility, accessible conformational space, and preferred 3D arrangements (low-energy conformations). As expected, the overall shape of both ligands did not change significantly on changing the simulation medium, as roughly determined by comparison of the dihedral angles, which define the overall shape of the molecules (see Figure S1, Supplementary Material). For **7d**, MD trajectories (300 and 600 K) showed that $\tau1$ and $\tau2$ adopted a trans conformation that is maintained throughout the simulations, while $\tau3$–$\tau5$ access different conformations (Figures S2 and S3, Supplementary Material). Overall, the molecule adopted an elongated cylindrical shape (Figure S4, Supplementary Material). In particular, the conformational behaviour of dihedrals $\tau1$ and $\tau4$ seems to be quite important (vide infra), given that the endocyclic C = O at position 5 appears to be involved in the catalytic process, while the closest C = O group could play an important role in anchoring to the subpocket of the binding site[40]. The superimposition (Figure 2, panel A) of the minimised conformers of **7d** extracted from the MD trajectory ($T = 600$ K, $\varepsilon = 4r$), which are comprised within about 2 kcal mol^{-1}, exemplifies the conformational space accessible to the molecule through rotations about the $\tau3$–$\tau5$ dihedrals.

Compound **8d** appears to be a little bit more flexible compared to **7d**, as suggested by the larger variability of the distance separating the centroids of the phenyl rings. While the $\tau1$, $\tau2$, and $\tau3$ dihedrals were almost frozen irrespective of the simulation temperature and medium [they adopted cis, trans (with only few exceptions), and cis (with only few exceptions) conformations, respectively], increasing the temperature from 300 to 600 K made the $\tau5$ and $\tau6$ dihedrals freely rotate (Figures S5 and S6, Supplementary Material). Dihedral $\tau4$ showed a preference for a gauche arrangement. Overall, **8d** is V-shaped: in most cases both of the phenyl rings were rotated with respect to the mean plane defined by the heterocyclic ring (Figure S7, Supplementary Material). The superimposition (Figure 2, panel B) of the minimised conformers of **8d** extracted from MD simulations ($T = 600$ K, $\varepsilon = 4r$) revealed two possible orientations for the carbonyl group of the ester function at position 5, which is supposed to be involved in

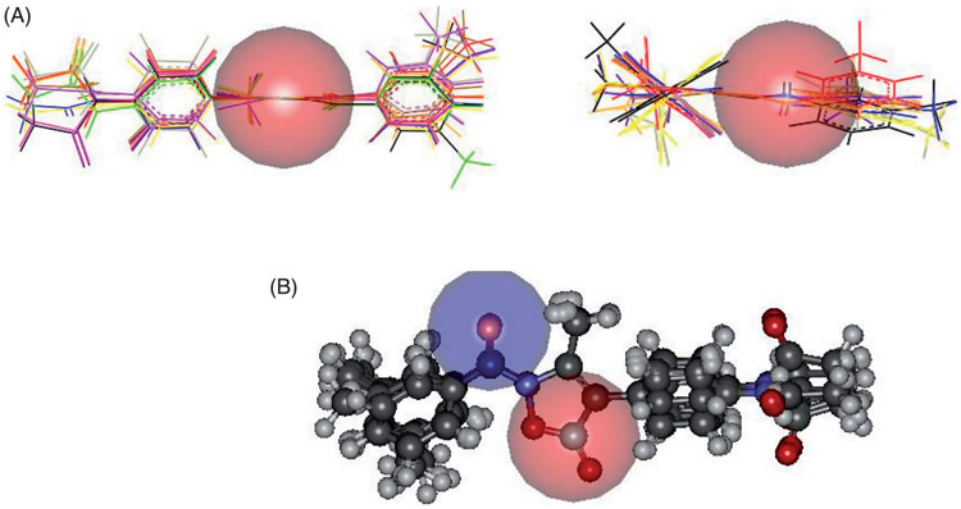

Figure 3. Panel (A): Accessibility of the carbonyl grouping involved in the catalytic process estimated by the dimension of a sphere (in red, $r = 2.5$ Å) centred on the carbon atom of **7d** (left) and **8d** (right). Panel (B): Accessibilities of the carbonyl groups in **7d** involved in the catalytic process and in H-bond interactions with the receptor points estimated by the dimension of a sphere centred on the carbon and oxygen atom ($r = 2.5$ Å, red and blue, respectively).

the catalytic process (energies are comprised within about 5 kcal mol^{-1}).

In both inhibitors, accessibility of the carbonyl group involved in the catalytic process was roughly estimated by the dimension of a sphere centred on the C = O carbon atom ($r = 2.5$ Å, in red in Figure 3, panel A). Similarly a sphere ($r = 2.5$ Å, in blue in Figure 3, panel B) centred on the oxygen atom, which could be involved in H-bond interactions with the receptor points, was used to assess the exposure to the environment of C = O in **7d**. Panel A of Figure 3 suggests a more crowded region about the site of the nucleophilic attack of **8d**, which could account for its lower activity compared to **7d** (in **8d**, the carbonyl group is directly bound to the phenyl ring and faces the pending arm at position 4). In addition, the almost cylindrical shape of **7d** caused, at least in principle, the carbonyl carbon atom to be attacked from both the side of the plane defined by the 5-membered ring (Figure S8, Supplementary Material). In contrast, only one side of the ester group in **8d** appeared to be easily accessible to the hydroxyl group of Ser195 (Figure S9, Supplementary Material). Finally, in both cases the terminal amide group appeared to be well exposed and thus prone for anchoring to the sub-pocket of the binding site.

Two different approaches were used to gain an idea of the interaction of **7d** and **8d** with HNE. First, docking of the inhibitors (two different starting conformations were considered) into the active site of HNE using the CDocker protocol (in vacuum, target temperature 300 K, 20 poses retained) and secondly, MD simulations on each inhibitor-HNE complex (in vacuum, simulation time 5 ns, $T = 300$K, with the atoms outside the binding sphere constrained to fixed points in space in order to save computational time). The structure of HNE complexed with a peptide chloromethyl ketone inhibitor was used for the docking study and MD simulations (1HNE[70] entry of the Protein Data Bank). The binding site of HNE was defined as a sphere with a 12 Å radius centred at the centroid of the five-membered ring of the peptide chloromethyl ketone inhibitor which covered all the active site amino acids of the HNE enzyme. All water molecules and bound inhibitor were removed from the macromolecule and hydrogen atoms were added.

Interaction energies from docking protocols on **7d** and **8d** with HNE did not significantly differ, and the two inhibitors showed comparable binding modes. In particular for **8d**, most of the saved poses featured Gly193 as the anchor group, and the H-bond interaction with this amino acid pushed the site of the nucleophilic attack quite distant from Ser195. However, a few poses show Gly193 involved as an H-bond donor to the ester function of **8d** and, in these cases, the distance HO(Ser195) … CO ranged from 3.3 to 4.8 Å (Figure 4, Panel A). The same amino acids are also involved in the interaction with **7d**. Anchoring of the terminal NHCO group to Ser195 *via* H-bonds pushed the CO at position 5 distant from the nucleophilic –OH of Ser195, while H-bonds between 5-CO and Gly193 brought the two partners of the nucleophilic attack a little bit closer (distances range from 4.3 to 5.1 Å, Figure 4, Panel B). However, the mean distance between the inhibitor-HNE reacting sites, as determined from the saved poses, was very long for both complexes (ca 7 Å).

In summary, docking results do not help to explain the different activities of the two inhibitors towards HNE. The fact that the CDocker protocol keeps the receptor rigid, while the inhibitor is allowed to flex during the refinement, could however significantly affect the results, and this is the reason why the ligand–receptor binding affinity was also assessed by MD. On the other hand, MD simulations confirmed the leading role of Gly193 as an anchoring group for both inhibitors. However, in contrast with the docking results, MD shows the 5-CO grouping of **7d** was significantly closer to the HNE reactive site (distance less than 4.5 Å in a large fraction of the snapshot conformations) with respect to the corresponding active site of **8d** ($d < 5$ Å in few of the sampled conformations). In contrast, a comparison of the total number of the intermolecular DH … A contacts (distances less than 2.5 Å) shows a greater propensity for **8d** to form H-bond interactions compared to **7d**. In addition, while multiple intermolecular H-bonds were present for **8d**, most of the snapshot conformations of **7d** exhibited only one H-bond interaction. In other words, the net of intermolecular H-bonds that involves **8d** keeps the molecule quite distant from Ser195. Finally, it is noteworthy that in the HNE complexes with **8d** featuring closer distances between the active sites, the heteroatoms of the 5-membered ring acted as H-bond acceptors both towards the Ser195 –OH group and Gly193. As a result of these interactions, the relative 3 D arrangement of **8d** in the HNE active site does not appear to be propitious for approach of the nucleophile of Ser195 (see for example Figure 5, Panel A). In contrast, the H-bond between 5-CO and Gly193, which in most cases held

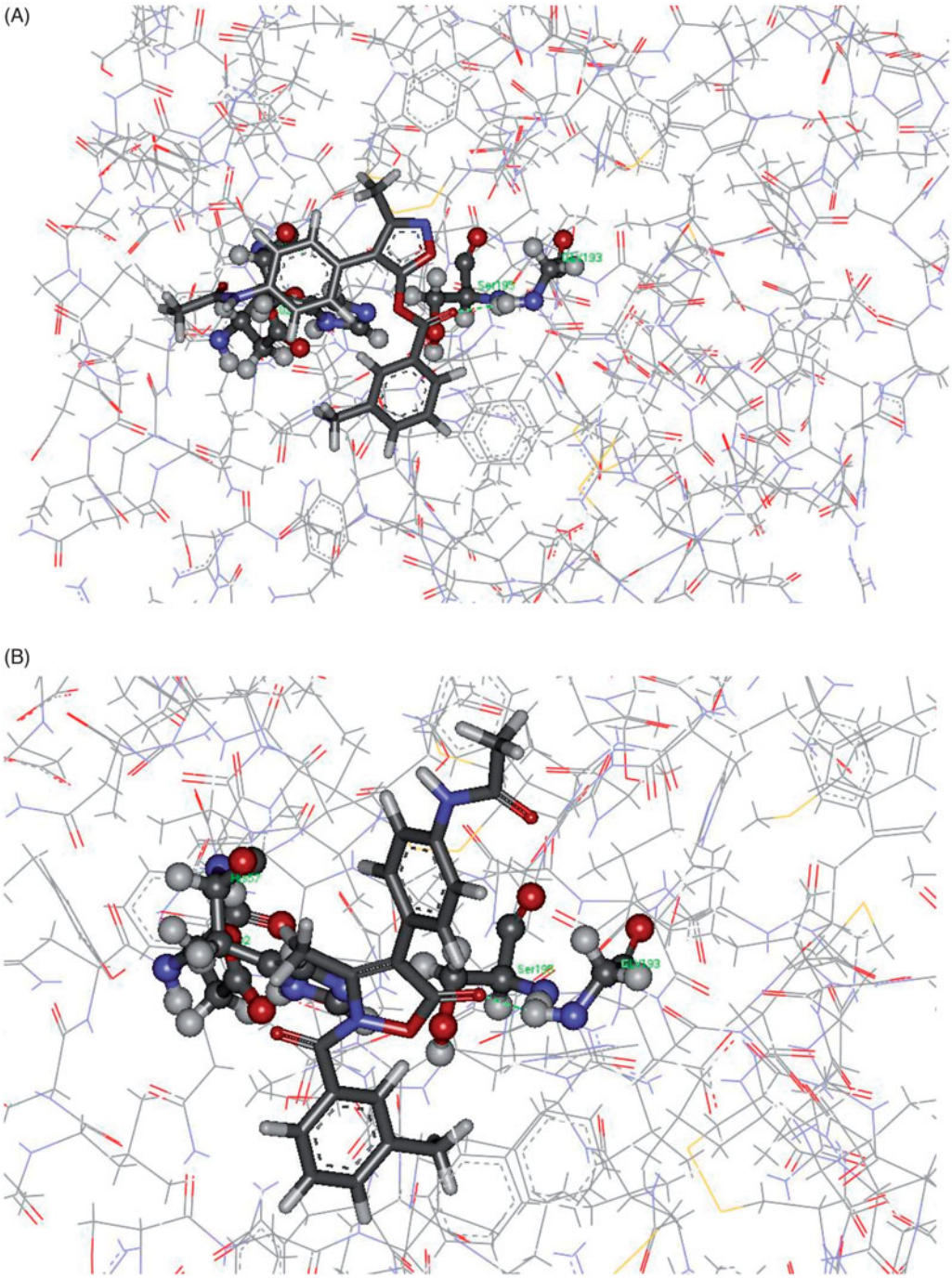

Figure 4. Panel (A): Pose from the CDocker protocol showing Gly193 involved as H-bond donor to the carbonyl function of **8d**. Panel (B): Pose from the CDocker protocol showing Gly193 involved as H-bond donor to 5-CO in **7d**.

together the **7d**/HNE adduct, results in a favourable 3 D arrangement of the reacting partners (see for example Figure 5, panel B) for nucleophilic attack.

Stability and kinetic features

The most potent isoxazolones with $IC_{50} < 100$ nM and their ester analogs were further evaluated for chemical stability in aqueous buffer using spectrophotometry to detect compound hydrolysis. The compounds had $t_{1/2}$ values from 2.9 to 9.6 h for spontaneous hydrolysis, indicating that the amides were more stable than the esters in the corresponding pairs of **7a/8a**, **7d/8d**, and **7e/8e** (Table 4). In general, the isoxazolones were more stable than our previously described HNE inhibitors with cinnolinone[39], N-benzoylindazole[36,37], and N-benzoylpyrazole scaffolds[71].

The most potent isoxazolones were also selected for evaluation of the reversibility of HNE inhibition over time. As shown in Figure 6, HNE inhibition was rapidly (~30 min) reversed for compounds **7d** and **7b**. The inhibition was maximal for up to 60 min with compound **7e** and >120 min for the other tested compounds (**4a**, **4b**, and **7a**). However, inhibition by the compounds was eventually reversed, and full recovery of HNE activity was observed by 4 h after treatment with 8 μM of the compound (e.g. see Figure 6).

To better understand the mechanism of action of these isoxazolone HNE inhibitors, we performed kinetic experiments. As

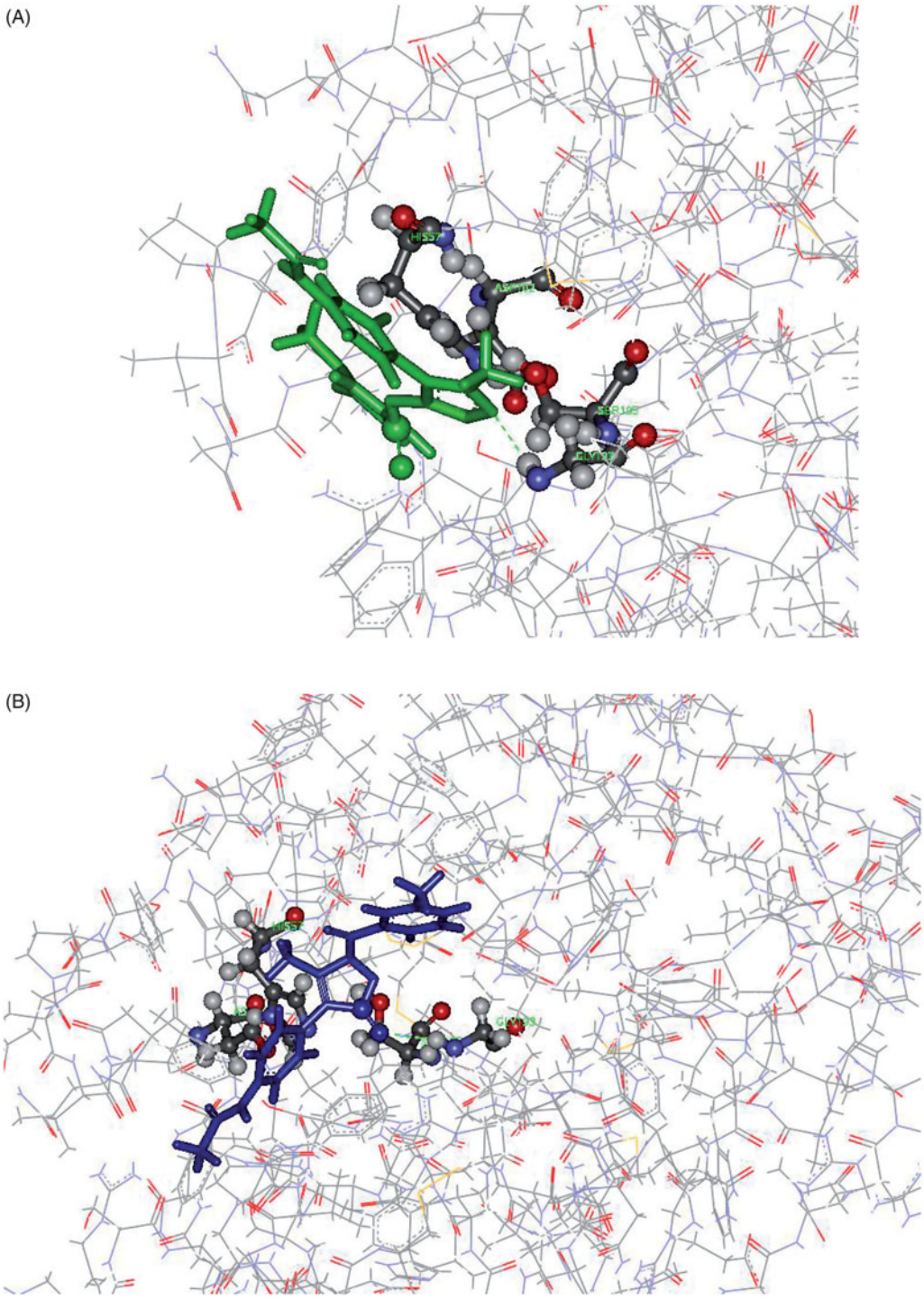

Figure 5. Panel (A): View of the **8d**-HNE adduct from MD showing the H-bond interaction between the nitrogen atom of the 5-membered ring acting as H-bond acceptor towards Gly193. Panel (B): View of the **7d**-HNE adduct from MD showing the H-bond interaction between the oxygen of 5-CO acting as H-bond acceptor towards Gly193.

shown in Figure 7, the representative double-reciprocal Lineweaver–Burk plot of fluorogenic substrate hydrolysis by HNE in the absence and presence of compounds **7d** and **8d** indicates that these compounds are competitive HNE inhibitors.

Conclusions

In the present study, we report a new series of isoxazolones as potent HNE inhibitors, confirming our previous results[40], which indicated this nucleus as an appropriate scaffold for this target. The most potent compounds had a methyl group at position 3 and a (substituted)phenyl ring at position 4, and the higher HNE inhibitory activity was found for compound **7a** ($IC_{50} = 20$ nM). In addition to the 2-NCO derivatives, a number of 5-NCO compounds were obtained, although with lower activity than the corresponding amide. Studies of chemical stability in aqueous buffer indicated that amides were generally more stable than esters, while kinetic experiments confirmed that both amides and esters were

Table 4. Half-life ($t_{1/2}$) for the spontaneous hydrolysis of selected derivatives.

Comp.	$t_{1/2}$ (h)	Absorbance (nm)[a]
4a	4.1	330
4b	8.3	290
7a	7.7	340
8a	5.3	320
7d	3.9	340
8d	2.9	330
7e	9.6	320
8e	5.6	280

[a]Absorption used for monitoring spontaneous hydrolysis.

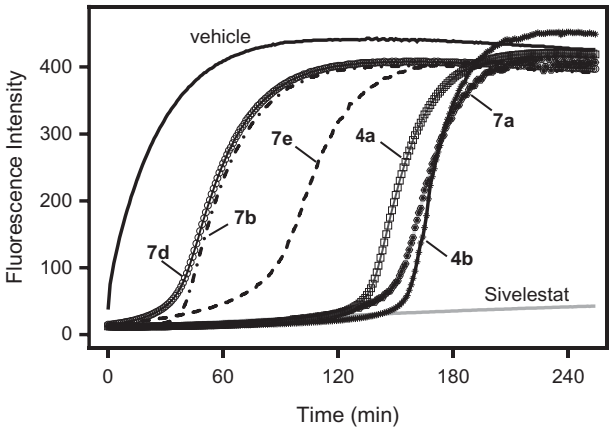

Figure 6. Evaluation of HNE inhibition by representative isoxazolones and Sivelestat over extended periods of time. HNE was incubated with the indicated compounds (8 μM), and kinetic curves monitoring substrate cleavage catalysed by HNE over time are shown. Representative curves are from two independent experiments.

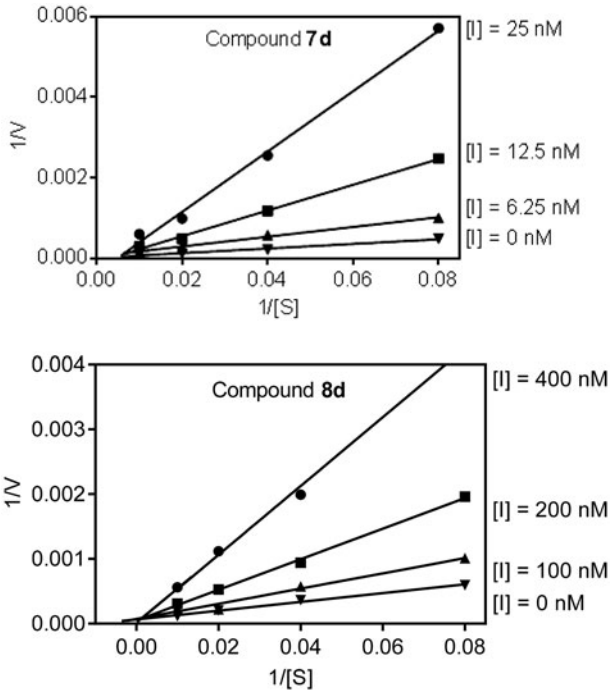

Figure 7. Kinetics of HNE inhibition by compounds **7d** and **8d**. Representative double reciprocal Lineweaver–Burk plots are shown from three independent experiments.

competitive HNE inhibitors. Docking and molecular dynamics studies are the different approaches used to understand the interactions of the two isomers **7d** and **8d** with HNE. Both studies highlight the fundamental role of Gly193 as anchoring group for both the inhibitors, but the MD simulations help us to explain the difference in inhibitory activity between the inhibitors **7d** and **8d**. The ester isomer **8d** shows a greater propensity to form H-bond interactions with respect to **7d** and as a result the molecule is quite distant from the Ser195, the amino acid responsible for the nucleophilic attack. While the amide isomer **7b** appears more mobile within the active site of HNE, being held in place by single H-bond interactions (vs. multiple in **8d**), which leads the C = O at position 5 to obtain a favourable orientation for the nucleophilic attack by Ser195.

Disclosure statement

No potential conflict of interest was reported by the authors.

Funding

This research was supported in part by National Institutes of Health IDeA Program COBRE Grant GM110732; USDA National Institute of Food and Agriculture Hatch project 1009546; the Ministry of Education and Science of the Russian Federation (project No. 4.8192.2017), Montana University System Research Initiative: 51040-MUSRI2015–03; Montana State University Agricultural Experiment Station.

ORCID

Maria Paola Giovannoni http://orcid.org/0000-0003-0310-7850
Igor A. Schepetkin http://orcid.org/0000-0003-2139-8110
Mark T. Quinn http://orcid.org/0000-0001-8114-5073
Gabriella Guerrini http://orcid.org/0000-0001-6711-7965
Paola Paoli http://orcid.org/0000-0002-2408-4590
Patrizia Rossi http://orcid.org/0000-0002-6316-338X
Gianluca Bartolucci http://orcid.org/0000-0002-5631-8769
Claudia Vergelli http://orcid.org/0000-0001-9774-8047

References

1. Brocklehurst K, Willenbrock F, Salih E. In: Neuberger A, Brocklehurst K, eds. New comprehensive biochemistry. Amsterdam: Elsevier; 1987;16:39–158.
2. Hedstrom L. Serine protease mechanism and specificity. Chem Rev 2002;102:4501–23.
3. Rawling ND, Morton FR, Kok CY, et al. MEROPS: the peptidase database. Nucleic Acids Res 2007;36:D320–5.
4. Perera NC, Schilling O, Kittel H, et al. NSP4, an elastase-related protease in human neutrophils with arginine specificity. Proc Natl Acad Sci USA 2012;109:6229–34.
5. Korkmaz B, Horwitz MS, Jenne DE, Gauthier F. Neutrophil elastase, proteinase 3, and cathepsin G as therapeutic targets in human diseases. Pharmacol Rev 2010;62:726–59.
6. Heutinck KM, ten Berge IJ, Hack CE, et al. Serine proteases of the human immune system in health and disease. Mol Immunol 2010;47:1943–55.
7. Bardoel BW, Kenny EF, Sollberger G, Zychlinsky A. The balancing act of neutrophils. Cell Host Microbe 2014;15:526–36.

8. Sinha S, Watorek W, Karr S, et al. Primary structure of human neutrophil elastase. Proc Natl Acad Sci USA 1987;84:2228–32.
9. Chua F, Laurent GJ. Neutrophil elastase: mediator of extracellular matrix destruction and accumulation. Proc Am Thorac Soc 2006;3:424–7.
10. Pham CT. Neutrophil serine proteases: specific regulators of inflammation. Nat Rev Immunol 2006;6:541–50.
11. Stapels DA, Geisbrecht BV, Rooijakkers SH. Neutrophil serine proteases in antibacterial defense. Curr Opin Microbiol 2015;23:42–8.
12. Saitoh T, Komano J, Saitoh Y, et al. Neutrophil extracellular traps mediate a host defense response to human immunodeficiency virus-1. Cell Host Microbe 2012;12:109–16.
13. Fitch PM, Roghanian A, Howie SEM, Sallenave J-M. Human neutrophil elastase inhibitors in innate and adaptive immunity. Biochem Soc Trans 2006;34:279–82.
14. Janciauskiene SM, Bals R, Koczulla R, et al. The discovery of α1-antitrypsin and its role in health and disease. Respir Med 2011;105:1129–39.
15. Quabius ES, Görögh T, Fischer GS, et al. The antileukoprotease secretory leukocyte protease inhibitor (SLPI) and its role in the prevention of HPV-infections in head and neck squamous cell carcinoma. Cancer Lett 2015;357:339–45.
16. Zhong QQ, Wang X, Li YF, et al. Secretory leukocyte protease inhibitor promising protective roles in obesity-associated atherosclerosis. Exp Biol Med 2017;242:250–7.
17. Zani M-Z, Nobar SM, Lacour SA, et al. Kinetics of the inhibition of neutrophil proteinases by recombinant elafin and pre-elafin (trappin-2) expressed in *Pichia pastoris*. Eur J Biochem 2004;271:2370–8.
18. Kawabata K, Hagio T, Matsuoka S. The role of neutrophil elastase in acute lung injury. Eur J Pharmacol 2002;451:1–10.
19. Barnes PJ, Stockley RA. COPD: current therapeutic interventions and future approaches. Eur Respir J 2005;25:1084–106.
20. Pandey KC, De S, Mishra PK. Role of proteases in chronic obstructive pulmonary disease. Front Pharmacol 2017; 8:512–9.
21. Kelly E, Greene CM, McElvaney NG. Targeting neutrophil elastase in cystic fibrosis. Expert Opin Ther Targets 2008;12: 145–57.
22. Wagner CJ, Schultz C, Mall MA. Neutrophil elastase and matrix metalloproteinase 12 in cystic fibrosis lung disease. Mol Cell Pediatr 2016;3:25.
23. Hilbert N, Schiller J, Arnhold J, Arnold K. Cartilage degradation by stimulated human neutrophils: elastase is mainly responsible for cartilage damage. Bioorg Chem 2002; 30:119–32.
24. Henriksen PA, Sallenave J-M. Human neutrophil elastase: mediator and therapeutic target in atherosclerosis. Int J Biochem Cell Biol 2008;40:1095–100.
25. Dhanrajani PJ. Papillon–Lefevre syndrome: clinical presentation and a brief review. Oral Surg Oral Med Oral Pathol Oral Radiol Endod 2009;108:e1–7.
26. Cools-Lartigue J, Spicer J, Najmeh S, Ferri L. Neutrophil extracellular traps in cancer progression. Cell Mol Life Sci 2014; 71:4179–94.
27. Lucas SD, Costa E, Guedes RC, Moreira R. Targeting COPD: advances on low-molecular-weight inhibitors of human neutrophil elastase. Med Res Rev 2013;33:E73–101.
28. Tsai Y-F, Hwang T-L. Neutrophil elastase inhibitors: a patent review and potential applications for inflammatory lung diseases (2010–2014). Expert Opin Ther Pat 2015;25: 1145–58.
29. Tebbutt SJ. Technology evaluation: transgenic alpha-1-antitrypsin (AAT), PPL therapeutics. Curr Opin Mol Ther 2000;2: 199–204.
30. American Thoracic Society/European Respiratory Society Statement, Standards for the diagnosis and management of individual with alpha-1-antitrypsin deficiency. Am J Respir Crit Care Med 2003;168:818–900.
31. Von Nussbaum F, Li VMJ. Neutrophil elastase inhibitors for the treatment of (cardio)pulmonary diseases: into clinical testing with pre-adaptive pharmacophores. Bioorg Med Chem 2015;25:4370–81.
32. Ohbayashi H. Current synthetic inhibitors of human neutrophil elastase in 2005. Expert Opin Ther Pat 2005;15:759–71.
33. Iwata K, Doi A, Ohji G, et al. Effect of neutrophil elastase inhibitor (Sivelestat sodium) in the treatment of acute lung injury (ALI) and acute respiratory distress (ARDS): a systemic review and meta-analysis. Intern Med 2010;49:2423–32.
34. Stockley R, De Soyza A, Gunawardena K, et al. Phase II study of a neutrophil elastase inhibitor (AZD9668) in patients with bronchiectasis. Respir Med 2013;107:524–33.
35. Von Nussbaum F, Li VMJ, Allerheiligen S, et al. Freezing the bioactive conformation to boost potency: the identification of BAY 85-8501, a selective and potent inhibitor of human neutrophil elastase for pulmonary diseases. ChemMedChem 2015;10:1163–73.
36. Crocetti L, Giovannoni MP, Schepetkin IA, et al. Design, synthesis and evaluation of N-benzoylindazole derivatives and analogues as inhibitors of human neutrophil elastase. Bioorg Med Chem 2011;19:4460–72.
37. Crocetti L, Schepetkin IA, Cilibrizzi A, et al. Optimization of N-benzoylindazole derivatives as inhibitors of human neutrophil elastase. J Med Chem 2013;56:6259–72.
38. Crocetti L, Schepetkin IA, Ciciani G, et al. Synthesis and pharmacological evaluation of indole derivatives as deaza analogues of potent human neutrophil elastase inhibitors. Drug Dev Res 2016;77:285–99.
39. Giovannoni MP, Schepetkin IA, Crocetti L, et al. Cinnoline derivatives as human neutrophil elastase inhibitors. J Enzyme Inhib Med Chem 2016;31:628–39.
40. Vergelli C, Schepetkin IA, Crocetti L, et al. Isoxazol-5(*2H*)-one: a new scaffold for potent human neutrophil elastase (HNE) inhibitors. J Enzyme Inhib Med Chem 2017;32:821–31.
41. Beccalli EM, Marchesini A. The Vilsmeier–Haack reaction of isoxazoline-5-ones. Synthesis and reactivity of 2-(dialkylamino)-1,3-oxazin-6-ones. J Org Chem 1987;52:3426–34.
42. Breslow T, Eicher A, Krebs RA, et al. Diphenylcyclopropenone. J Am Chem Soc 1965;87:1320–5.
43. Boulton AJ, Katritzky AR. The tautomerism of heteroaromatic compounds with five-membered rings-I: 5-hydroxyisoxazoles-isoxazol-5-ones. Tetrahedron 1961;12:41–50.
44. Batra S, Bhaduri AP. An account of the chemistry of 3,4-disubstituted 5-isoxazolones. J Indian Inst Sci 1994;74: 213–26.
45. Safi R, Rodriguez F, Hilal G, et al. Hemisynthesis, antitumoral effect, and molecular docking studies of ferutinin and its analogues. Chem Biol Drug Des 2016;87:382–97.
46. Onoda A, Yamada Y, Nakayama Y, et al. Stabilization of calcium- and terbium-carboxylate bonds by NH····O hydrogen bonds in a mononuclear complex. A functional model of the active site of calcium-binding proteins. Inorg Chem 2004;43:4447–55.
47. Belzecki C, Urbanski T. New antituberculosis agents. XXXVII. Thiosemicarbazones of oxo acids. 2. Thiosemicarbazones of aroyl fatty acids. Roczniki Chemii 1958;32:769–78.

48. Cadieux JA, Zhang Z, Mattice M, et al. Synthesis and biological evaluation of substituted pyrazoles as blockers of divalent metal transporter 1 (DMT1). Bioorg Med Chem Lett 2012;22:90–5.
49. Xie X, Cai G, Ma D. CuI/L-proline-catalyzed coupling reactions of aryl halides with activated methylene compounds. Org Lett 2005;7:4693–5.
50. Monastyrskyi A, Namelikonda NK, Manetsch R. Metal-free arylation of ethyl acetoacetate with hypervalent diaryliodonium salts: an immediate access to diverse 3-aryl-4(1H)-quinolones. J Org Chem 2015;80:2513–20.
51. Wierenga W, Evans BR, Zurenko G. Benzisoxazolones: antimicrobial and antileukemic activity. J Med Chem 1984;27:1212–5.
52. Forist AA, Weber DJ. Kinetics of hydrolysis of hypoglycemic 1-acyl 3,5-dimethylpyrazoles. J Pharm Sci 1973;62:318–9.
53. Accelrys Software Inc., San Diego, CA 92121, USA.
54. Brooks BR, Bruccoleri RE, Olafson BD, et al. CHARMM: a program for macromolecular energy, minimization, and dynamics calculations. J Comput Chem 1983;4:187–217.
55. Gaussian 09, Revision C.01, Frisch MJ, Trucks GW, Schlegel HB, Scuseria GE, Robb MA, Cheeseman JR, Scalmani G, Barone V, Mennucci B, Petersson GA, Nakatsuji H, Caricato M, Li X, Hratchian HP, Izmaylov AF, Bloino J, Zheng G, Sonnenberg JL, Hada M, Ehara M, Toyota K, Fukuda R, Hasegawa J, Ishida M, Nakajima T, Honda Y, Kitao O, Nakai H, Vreven T, Montgomery JA, Jr, Peralta JE, Ogliaro F, Bearpark M, Heyd JJ, Brothers E, Kudin KN, Staroverov VN, Keith T, Kobayashi R, Normand J, Raghavachari K, Rendell A, Burant JC, Iyengar SS, Tomasi J, Cossi M, Rega N, Millam JM, Klene M, Knox JE, Cross JB, Bakken V, Adamo C, Jaramillo J, Gomperts R, Stratmann RE, Yazyev O, Austin AJ, Cammi R, Pomelli C, Ochterski JW, Martin RL, Morokuma K, Zakrzewski VG, Voth GA, Salvador P, Dannenberg JJ, Dapprich S, Daniels AD, Farkas O, Foresman JB, Ortiz JV, Cioslowski J, Fox DJ, Gaussian, Inc., Wallingford CT, 2010.12.
56. Becke AD. Density-functional exchange-energy approximation with correct asymptotic behavior. Phys Rev 1988;38: 3098–100.
57. Vosko SH, Wilk L, Nusair M. Accurate spin-dependent electron liquid correlation energies for local spin density calculations: a critical analysis. Can J Phys 1980;58:1200–11.
58. Grimme SJ. Semiempirical GGA-type density functional constructed with a long-range dispersion correction. J Comput Chem 2006;27:1787–99.
59. Hehre WJ, Ditchfield R, Pople JA. Self-consistent molecular orbital methods. XII. Further extensions of Gaussian-type basis sets for use in molecular orbital studies of organic molecules. J Chem Phys 1972;56:2257–61.
60. Peng C, Ayala PY, Schlegel HB, Frisch MJ. Using redundant internal coordinates to optimize equilibrium geometries and transition states. J Comput Chem 1996;17:49–56.
61. Dassault Systèmes BIOVIA, Discovery Studio Visualizer, Release 4.5, San Diego: Dassault Systèmes; 2015.
62. Katritzky AR, Barczynski P, Ostercamp DL, Yousaf TI. Mechanisms of heterocyclic ring formations. 4. A ^{13}C-NMR study of the reaction of β-keto esters with hydroxylamine. J Org Chem 1986;51:4037–42.
63. Laufer SA, Margutti S. Isoxazolone based inhibitors of p38 MAP kinases. J Med Chem 2008;51:2580–4.
64. Franchini PF. Dipole moments and tautomerism of isoxazolin-5-ones. Corsie Sem Chim 1968;14:23–5.
65. Cencioni R, Franchini PF, Orienti M. Dipole moments of 5-substitued isoxazoles. I. Dipole moments and tautomerism of isoxazolin-5-one. Tetrahedron 1968;24:151–66.
66. Elguero J, Marzin C, Katritzky AR, Linda P, eds. Advances in heterocyclic chemistry, supplement 1, the tautomerism of heterocycles. New York: Academic Press; 1976:656.
67. Frolund B, Jensen LS, Guandalini L, et al. Potent 4-aryl- or 4-arylalkyl-substituted 3-isoxazolol GABAA antagonists: synthesis, pharmacology, and molecular modeling. J Med Chem 2005;48:427–39.
68. Nishiwaki N, Nogami T, Kawamura T, et al. One-pot synthesis of polyfunctionalised isoxazol(in)es. J Org Chem 1999; 64:6476–8.
69. Allen FH. The Cambridge Structural Database: a quarter of a million crystal structures and rising. Acta Crystallogr B 2002;58:380–8.
70. Navia MA, McKeever BM, Springer JP, et al. Structure of human neutrophil elastase in complex with a peptide chloromethyl ketone inhibitor at 1.84 Å resolution. Proc Natl Acad Sci USA 1989;86:7–11.
71. Schepetkin IA, Khlebnikov AI, Quinn MT. N-benzoylpyrazoles are novel small-molecule inhibitors of human neutrophil elastase. J Med Chem 2007;50:4928–38.